Journal of Applied Geophysics 68 (2009) 459–478

Contents lists available at ScienceDirect

Journal of Applied Geophysics

journal homepage: www.elsevier.com/locate/jappgeo

Electromagnetic sounding of geothermal zones

Viacheslav Spichak [a,*], Adele Manzella [b]

[a] Geoelectromagnetic Research Center IPE RAS, Troitsk, Russia
[b] Institute of Geosciences and Earth Resources, CNR, Via Moruzzi 1, 5614 Pisa, Italy

ARTICLE INFO

Article history:
Received 1 March 2008
Accepted 23 May 2008

Keywords:
Electromagnetic sounding
Geothermal zones
Resistivity
Temperature
Alteration mineralogy
Modeling
Inversion

ABSTRACT

Electromagnetic (EM) data provide a substantial contribution to the geophysical mapping and monitoring of geothermal reservoirs. This paper presents an up-to-date picture of the achievements of EM methods for geothermal exploration as they have emerged over the last few years. It has been proved that EM sounding of geothermal zones and distant monitoring macro-parameters of the reservoirs, fluid-filled faults and other elements of the geothermal system are possible provided that modern 3-D inversion is used along with techniques that reduce the effects of industrial and geological noise. In addition, geological and petrophysical data also need to be included in the analysis.

1. Introduction

A key issue in the exploration of geothermal systems is the geophysical detection and monitoring, at several kilometers of depth, of reservoirs. Over the past decade there has been a huge increase in time-lapse reservoir monitoring and the development of seismic methods such as repeated 3D surface seismic, surface-to-borehole vertical seismic profiling, and borehole-to-borehole cross well seismic. At the same time, electromagnetic (EM) methods have been extensively used to detect deep fluid circulation, since resistivity is very sensitive to the presence of brines. Thanks to improved methodologies and software, EM is now very affordable and logistically practical, and has become very popular. Seismic imaging, whilst being a powerful geological mapping tool, has not always led to a significant improvement in understanding the nature and composition of the deep structure of geothermal systems. In order to progress and reduce the cost of geothermal exploration and monitoring, resistivity needs to be included in the analysis, especially if it is combined and integrated with other geophysical data, particularly seismic. An up-to-date picture of the achievements of EM methods for geothermal exploration will help us to understand and apply modern techniques.

Geothermal resources are ideal targets for EM methods since they produce strong variations in underground electrical resistivity. Geothermal waters have high concentrations of dissolved salts, that result in conducting electrolytes within a rock matrix. The resistivities of both the electrolytes and the rock matrix (to a lesser extent) are temperature dependent in such a way that there is a large reduction in the bulk resistivity to increasing temperatures. The resulting resistivity is also related to the presence of clay minerals, and can be reduced considerably when clay minerals and clay-sized particles are broadly distributed. On the other hand, resistivity should be always considered with care. Experience has shown that the correlation between low resistivity and fluid concentration is not always correct since alteration minerals produce comparable, and often a greater reduction in resistivity. Moreover, although water-dominated geothermal systems have an associated low resistivity signature, the opposite is not true, and the analysis requires the inclusion of geological and, possibly, other geophysical data, in order to limit the uncertainties.

Many papers have been devoted to the study of geothermal areas by EM methods over the last 30 years (see review papers by Berktold (1983) and Meju (2002) and references therein). Recently a number of important achievements have been reported, especially in EM data interpretation, and they are reviewed in this paper. First we will summarize the conceptual models of geothermal areas, the main factors influencing rock resistivity, and how they are evaluated using EM data. We will then present the results of applying EM techniques to geothermal images, with particular focus on magnetotelluric techniques but also looking at other EM methods. We will consider different aspects of EM data interpretation, with emphasis on new approaches of 3-D data inversion. A special section will be devoted to the effects of fracturing, faulting and regional tectonics on the detectability of geothermal zones using EM methods. We will also discuss MT monitoring of the reservoir macro-parameters and methods for dealing with cultural and geological noises. We will

* Corresponding author.
E-mail addresses: v.spichak@ru.net, spichak@igemi.troitsk.ru (V. Spichak), manzella@igg.cnr.it (A. Manzella).

0926-9851/$ – see front matter.
doi:10.1016/j.jappgeo.2008.05.007

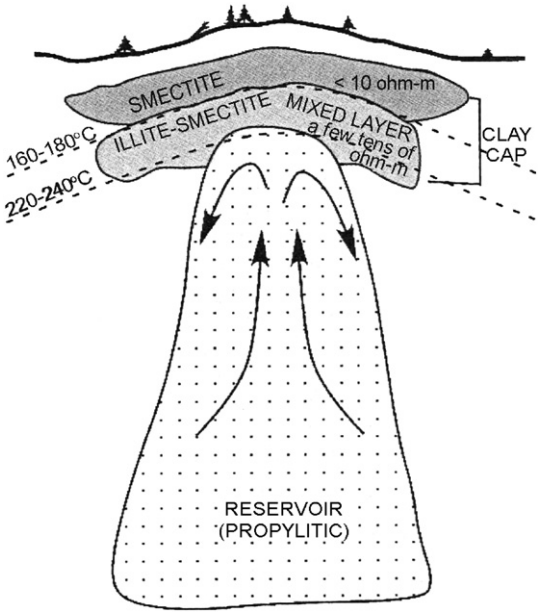

Fig. 1. Conceptual resistivity model of a convective geothermal system (after Oskooi et al., 2005).

address modern techniques of joint analysis and inversion of EM and other geophysical data, as well as the important practical problem of defining drilling targets depending on the type of geothermal zone. Finally, we will outline the latest contribution of EM sounding to geothermal exploration and the direction of future developments.

2. Conceptual models of geothermal areas

Geothermal resources are often confused with hydrothermal systems. By the latter we mean large amounts of hot, natural fluids contained in fractures and pores within rocks at temperatures above ambient level. Typically, when fluids are tapped at the surface either by natural manifestation or through drilling, hot water or steam is produced and its energy is converted into marketable products (electricity, process or space heat). A hydrothermal system is made up of three main elements: a heat source (very often represented by a magma chamber or intrusive bodies), a reservoir (i.e. a constituent host rock and the natural fluids contained in its fractures and pores), and a cap rock, i.e. a low permeability layer which restrains the main fluid flow at a depth where the temperature is high and is prevented from cooling by mixing with surface water. The sustainability of the system is guaranteed only when sufficient recharge through meteoric water is available, usually at a certain distance from the main, hot fluid circulation.

Geothermal resources refer to the thermal energy stored in the earth's crust. For many tens of years the geothermal community has tried to broaden the categories of geothermal systems beyond economically viable hydrothermal systems. The term EGS (enhanced or engineered geothermal system) is used nowadays to classify low permeability/porosity rock volumes at high temperatures that are stimulated (i.e. fractured) to extract economically justified amounts of heat. Another important frontier in geothermal research is linked to rocks that contain fluid in supercritical conditions, for which the conversion from thermal energy to mechanical energy would be particularly efficient. These different classes of geothermal resources have one parameter in common: temperature. Hence the primary aim of geothermal exploration is to map the temperature and heat. If there is a reasonable temperature at depth, geothermal explorers should be able to define the mineralogical composition of rocks, rheological conditions, but they are particularly interested in fluid pathways. All the aspects described so far have a direct effect on the resistivity distribution at depth.

Geothermal explorations have mainly been carried out in hydrothermal systems, which also applies to EM methods. Modern geothermal exploration, however, should be able to distinguish between different kinds of situations. The main difference between hydrothermal systems and other classes of geothermal resources is the rate of rock alteration, since hydrothermal systems are characterized by a prolonged water–rock interaction effect. Apart from this aspect, most of the following review, which refers primarily to hydrothermal systems, may be applied to any geothermal system.

In geothermal areas where the permeability is high and alteration pervasive, the conceptual model of the reservoir shown in Fig. 1 is appropriate. Reservoirs of this type have been found, for example, in Iceland, New Zealand, El Salvador, Djibouti, Indonesia and Japan (Árnason et al., 1986, 2000; Árnason and Flóvenz, 1995; Uchida, 1995; Oskooi et al., 2005; etc.). In this model, the lowest resistivity corresponds to a clay cap overlying the geothermal reservoir, while the resistivity of the reservoir itself may be much higher.

When topography is steep and a significant hydrological gradient is present in the subsurface, the overall structure of the geothermal system is more complex (Fig. 2). The conductive clay layer, e.g. smectite, may be quite deep over the system upflow and much closer to the surface in cooler outflow areas. In these cases, the resistivity anomaly at the surface is not centered over the geothermal reservoir (Anderson et al., 2000).

High-temperature geothermal systems, which are required for electric power production, usually occur where magma intrudes into high crustal levels (<10 km) and hydrothermal convection can take place above the intrusive body (e.g., Ander et al., 1984; Mogi and Nakama, 1993; Bai et al., 2001; Ushijima et al., 2005; Veeraswamy and Harinarayana, 2006; Zlotnicki et al., 2006). Fig. 3 reports a conceptual model showing the main elements of this type of geothermal system (Berktold, 1983).

3. Factors affecting resistivity of rocks

3.1. Temperature

Resistivity in hydrothermal areas is affected by vertically ascending, hot mineralised waters or gases that originate from the contact between groundwater and high-temperature intrusive magmas. The intrusions

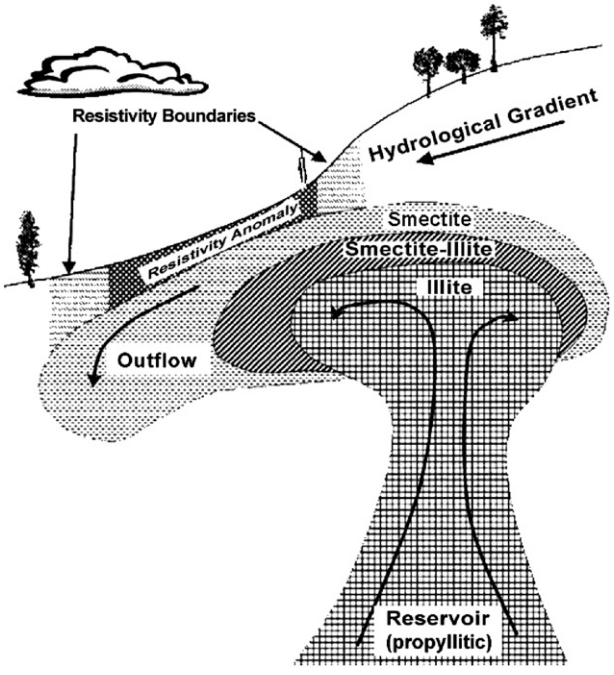

Fig. 2. A generalized geothermal system in a steep terrain (after Anderson et al., 2000).

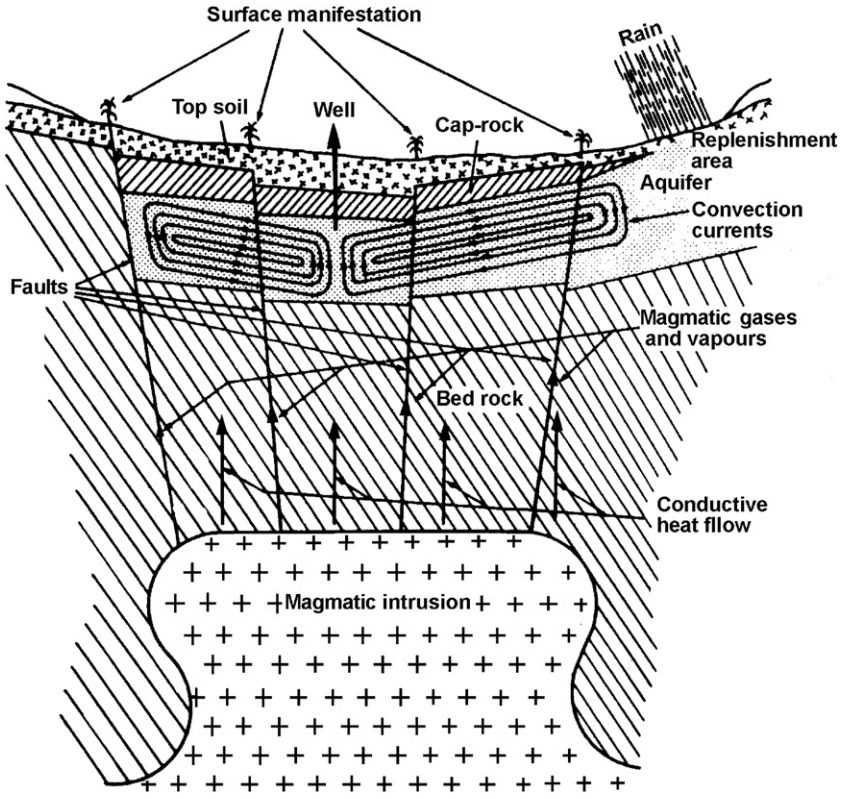

Fig. 3. Conceptual model of a hyper-thermal field (after Berktold, 1983).

themselves have a very low intrinsic resistivity at temperatures above approximately 800 °C (Bartel and Jacobson, 1987). In general, the melt composition, the fraction of partial melts and the presence of water greatly varies the resistivity of rocks (e.g. Lebedev and Khitarov, 1964; Wannamaker, 1986). For example, an electric resistivity of about 2 Ω m such as the one identified by Frischknecht (1967) in his study on Kilauea Iki lava lake molten basaltic magma or that of Hoffmann-Rothe et al. (2001) below Java, can be attributed either to molten basaltic magma at temperature >1250 °C, or to dry rhyolite at 950 °C, or a 1 wt.% H_2O melt at 875 °C, or a 3 wt.% H_2O melt at 830 °C or a 6 wt.% water-bearing melt at 760 °C. By increasing temperature and/or water content, resistivity may reduce to 0.1 Ω m.

The resistivity of a solid phase correlates with temperature and is documented in the laboratory through the semi-conductor equation:

$$\rho = \rho_0 e^{E/kT}, \tag{1}$$

where ρ_0 is the resistivity at a theoretically infinite temperature, E is an activation energy, k is a Boltzman constant, and T is an absolute temperature (K). When laboratory parameters and reasonable temperatures are used in the above relation it does not yield resistivities as small as those obtained from field measurements. For instance, Flóvenz et al. (1985) use the following empirical relation between the resistivity of altered basalts and temperature:

$$\rho_T = \rho_0 / (1 + \alpha(T - T_0))(1 + \beta(T - T_0)), \tag{2}$$

where ρ_T and ρ_0 are the resistivities at temperature T and reference temperature T_0. Empirical constants α and β are determined at T_0. This empirical relationship for resistivity exhibits about twice as much temperature dependency compared to electrolytic conduction alone. Flóvenz and Karlsdottir (2000) explain this by interface conduction along very thin but highly conductive films of clay minerals covering the interconnected micro-cracks in the rock.

3.2. Rock porosity and permeability

A quantitative empirical relation between the electric conductivity (the reciprocal of resistivity) of rocks and their porosity was first established by Archie (1942). A later formulation by Waxman and

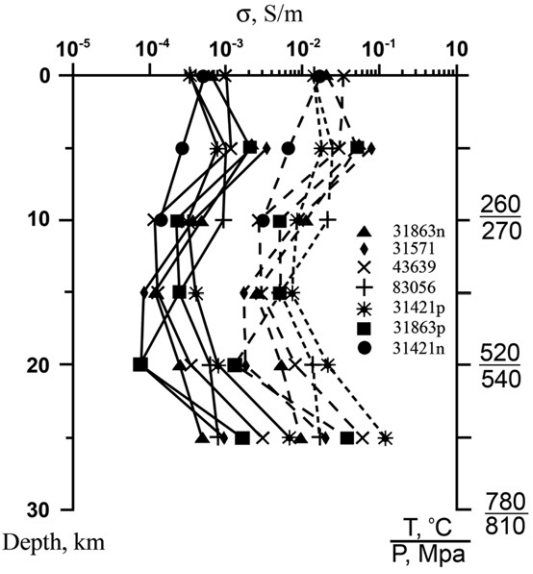

Fig. 4. Calculated values of electric conductivity of rocks with a fluid represented by a 0.1 M solution of NaCl (symbols are linked by solid lines) and 3.3 M solution of KCl (symbols are linked by dash lines) for regions with high heat flows (heat gradient 26°C/km). Electric conductivity (σ_r) is given in logarithmic scale. Symbols p and n at rock sample numbers indicate that in calculations the data on permeability in the directions parallel and perpendicular to the bedding, respectively, were used (after Shmonov et al., 2000).

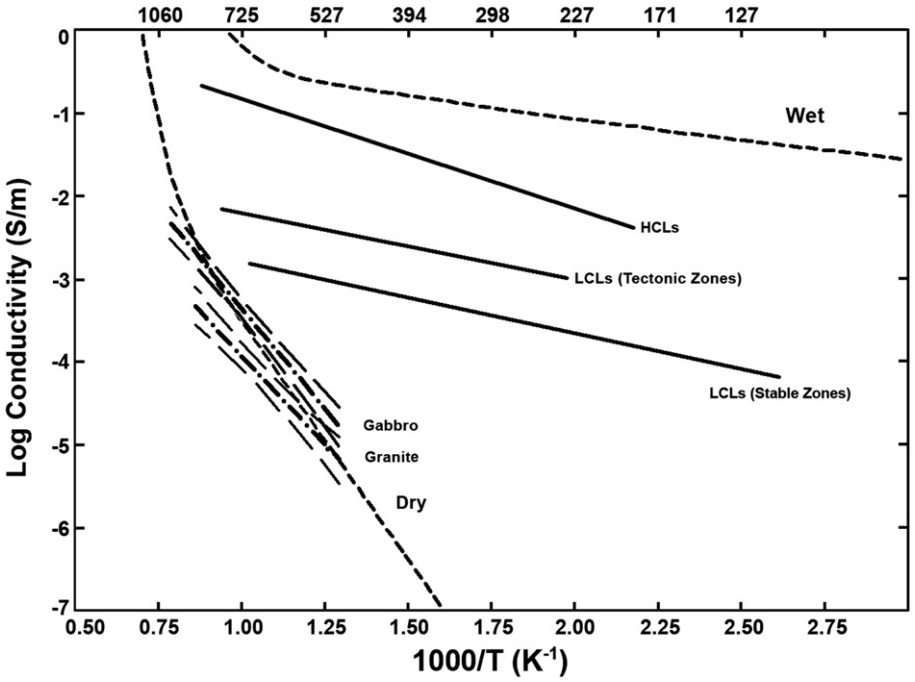

Fig. 5. Field conductivity–temperature (FCT) curves compared with laboratory measurements of conductivity in "dry" granite and "wet" granite with 1–2% water (short dashed lines). Also shown are laboratory measurements of conductivity in dry crustal rocks (dot-dash lines with 95% confidence limits shown as long dashed lines (after Shankland and Ander, 1983).

Smith (1968) allows for an additional conductivity contribution called surface conductivity σ_s. This formulation is

$$\sigma_r = (1/F)\sigma_w + \sigma_s \quad (3)$$

where σ_r is the bulk electric conductivity of a rock, σ_w is the electric conductivity of a saturating fluid, and F is the formation factor of the sample. In practice, if the ionic concentration of the solution is higher than 0.01 M, the contribution of surface conductivity in Eq. (3) can be neglected (Shmonov et al., 2000).

The formation factor F was expressed by Archie (1942) in terms of the fractional porosity ϕ as $F=\phi^{-m}$, where m is the cementation factor varying from 1.4 to 2.2 and often taken to be equal to 2. With this substitution the electric conductivity of a fluid-saturated rock is approximately

$$\sigma_r = \sigma_w \phi^2 \quad (4)$$

If the interconnected pore spaces are not damaged in the course of rock deformation, the hydrologic permeability k can be expressed by the relation (Zang et al., 1994)

$$k = \alpha\phi^3 \quad (5)$$

Coefficient α in Eq. (5) has a value of 1×10^{-12} m^2. Combining Eqs. (4) and (5), the electric conductivity of a rock can be estimated from the electric conductivity of a solution and the hydrologic permeability from the relation

$$\sigma_r = \sigma_w (k/\alpha)^{2/3} \quad (6)$$

Electric conductivity of a fluid increases as a function of temperature and pressure, whereas permeability can both decrease and increase with respect to these variables. But at low and moderate temperatures the expected variations in k or σ do not result in sharp conductivity increases with depth. In fact, at depths of more than 15 km the rock electric conductivity often decreases. This occurs because the permeability of rocks decreases due to compaction and temperature dependent plasticity (Shmonov et al., 2000).

Electric conductivity values of the order of 10^{-1} S/m can be reached in regions with high heat flows at depths of about 20 km where temperatures higher than 500 °C occur (Shmonov et al., 2000) (Fig. 4). In this case electric conductivity changes from ~0.001 to 0.05 S/m are expected at depths from 20 to 25 km (e.g. rock sample 31863p in Fig. 4). Such a rapid increase in electric conductivity (~0.0116 S/m km) produces "conductivity jumps" that provide excellent targets for EM soundings.

3.3. Clay minerals

Resistivity in geothermal areas is also governed to a great extent by the presence of hydrothermal alteration products including clay minerals. Clays are found in natural environments due to low-grade metamorphic and hydrothermal conditions. Systematic petrological, mineralogical, chemical and well-logging studies have been performed in recent years to investigate different hydrothermal alteration zones from the surface to great depths in geothermal fields worldwide. Temperature is the major control of clay mineralogy. Below the cool, unaltered shallow part of the earth, the environment is characterized by low temperature clay minerals such as smectite and zeolites. Both are electrically conductive and formed at temperatures above 70 °C. At higher temperatures, chlorite (more abundant in basaltic rocks) and/or illite (a less conductive clay mineral in acidic rocks) may appear, inter-layered with low temperature alteration minerals. The proportion of chlorite or illite increases with temperature, especially above 180 °C. Zeolites and smectite disappear at 220–240 °C and pure chlorite and/or illite usually appear at temperatures higher than 240 °C, along with other high-temperature alteration minerals such as epidote in propylitic alteration assemblages (e.g. Patrier et al., 1996; Fulignati et al., 1997; Gonzalez-Partida et al., 1997; Gianelli et al., 1998; Srodon, 1999; Lackschewitz et al., 2000; Gonzalez-Partida et al., 2000; Okada et al., 2000; Sener and Gevrek, 2000; Yang et al., 2000; Suharno et al., 2000; Natland and Dick, 2001; Yang et al., 2001).

If a rock contains clay minerals, then an extra conduction pathway is possible via the electrical double layer that forms at the interface of the

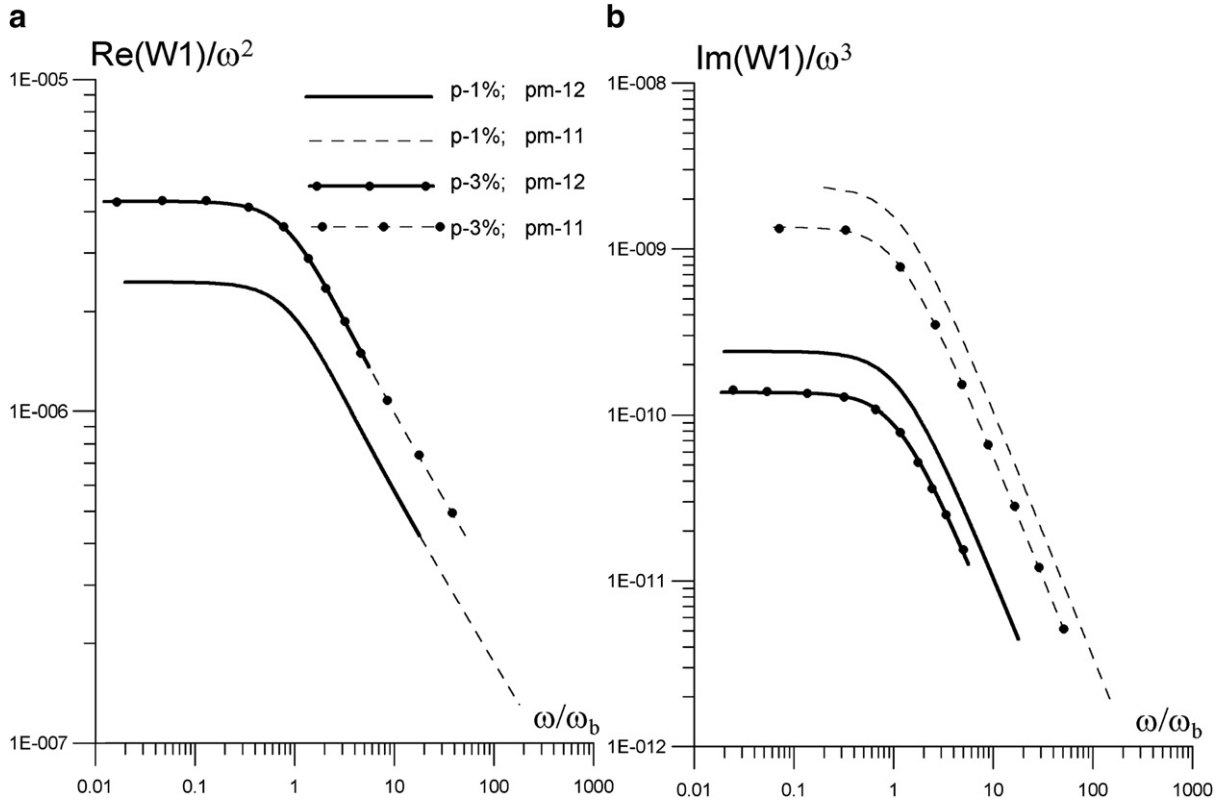

Fig. 6. Frequency dependences of real (a) and imaginary (b) parts of seismoelectric transfer function for different values of porosity and permeability; p — porosity, pm — permeability (after Svetov, 2006).

clay mineral and the water (for a more detailed discussion see Ward, 1990). This allows ions to move through the system with a lower effective viscosity than in the liquid phase. Such an additional contribution to the conductivity is referred to as surface conductivity or the double layer effect. It can exceed the conductivity of the water itself by many times and is thus of utmost importance in clay-rich zones.

Ussher et al. (2000) discussed the effect of clay minerals on surface electric conductivity. According to the authors, there are two conduction paths through clay-rich sediments: 1) via pore water and 2) a double layer of cations (also called the Gouy layer) which occurs in water at the interface of clay minerals. An analogue of this is an electrical circuit with two parallel paths as expressed by (3).

In general surface electric conductivity is determined as

$$\sigma_s = BQ_V, \tag{7}$$

where B is the equivalent conductance of counter ions (a function of solution conductivity), and Q_V is defined by

$$Q_V = \mathrm{CEC}(1-\phi)\rho_m\phi^{-1} \tag{8}$$

where ρ_m is matrix grain density and CEC is the cation exchange capacity of the clay present (in meq/gm).

In clay-rich rocks and where the pore water has low salinity, the bulk electric conductivity of the rock is proportional to the CEC of the clays. The role of this conduction mechanism in geothermal exploration was studied by Flóvenz et al. (2005). The authors conclude that for almost all freshwater-saturated high-temperature geothermal fields interface conduction is the dominant conduction mechanism, both in the chlorite and smectite zones. Thus, the observed decrease in resistivity at the top of a mixed clay/chlorite zone in many high-temperature geothermal reservoirs worldwide is most likely due to a much higher cation exchange capacity in smectites than in the alteration minerals below.

The effect of surface conductivity is generally more important when the water conductivity, therefore the intrinsic ion content, or the porosity or permeability is low. For example, when permeability is supported by a few main fractures and faults, such as in the Amiata area in Italy, then alteration minerals are localized, and the decrease in resistivity is mainly caused by the presence of hydrothermal fluids and partial melt (Volpi et al., 2003).

4. Evaluation of the temperature, porosity, permeability and alteration mineralogy using EM data

Electromagnetic, and in particular magnetotelluric sounding is a direct method for *in situ* studies of the structure and fluid circulation in the Earth's crust. Due to theoretical relations between the electric resistivity, on the one hand, and temperature, porosity, permeability and CEC formed by the presence of alteration minerals, on the other hand (see formulas (1)–(8) above), it is often used for the indirect estimation of these parameters.

4.1. Temperature

Shankland and Ander (1983) studied the correlation between the electric resistivity of high-conductivity layers (HCL) in the earth's crust detected using deep magnetotelluric sounding and the corresponding temperature values revealed from the heat flow data in different tectonic regions (Fig. 5). The authors concluded that, thanks to the relation between resistivity and temperature (FCT curves), electric resistivity profiles could be used to estimate regional geotherms.

Flóvenz and Karlsdottir (2000) studied the dependence of the resistivity of the low resistivity layer revealed by a transient electromagnetic (TEM) survey on the temperature estimated from borehole temperature logs. The authors observed a good correlation between resistivity and temperature, in agreement with the empirical relation (2). Harinarayana et al. (2006) also found a good correlation between the temperature and resistivity defined by MT sounding down to a depth of 2 km in the Puga geothermal field.

Spichak et al. (2007c) studied the relations between the temperature well logs and electrical conductivity profiles revealed by MT soundings in the tectonically active area of northern Tien Shan. It was shown that the use of electrical conductivity data in addition to temperature records may essentially decrease temperature assessment errors (up to two times, if the number of wells used is less than 8–10). Based on their findings, the authors proposed using electrical conductivity from MT measurements in geothermal areas for indirect temperature estimations.

4.2. Porosity and permeability

Direct evaluation of rock porosity and permeability from EM sounding data would significantly facilitate geothermal exploration

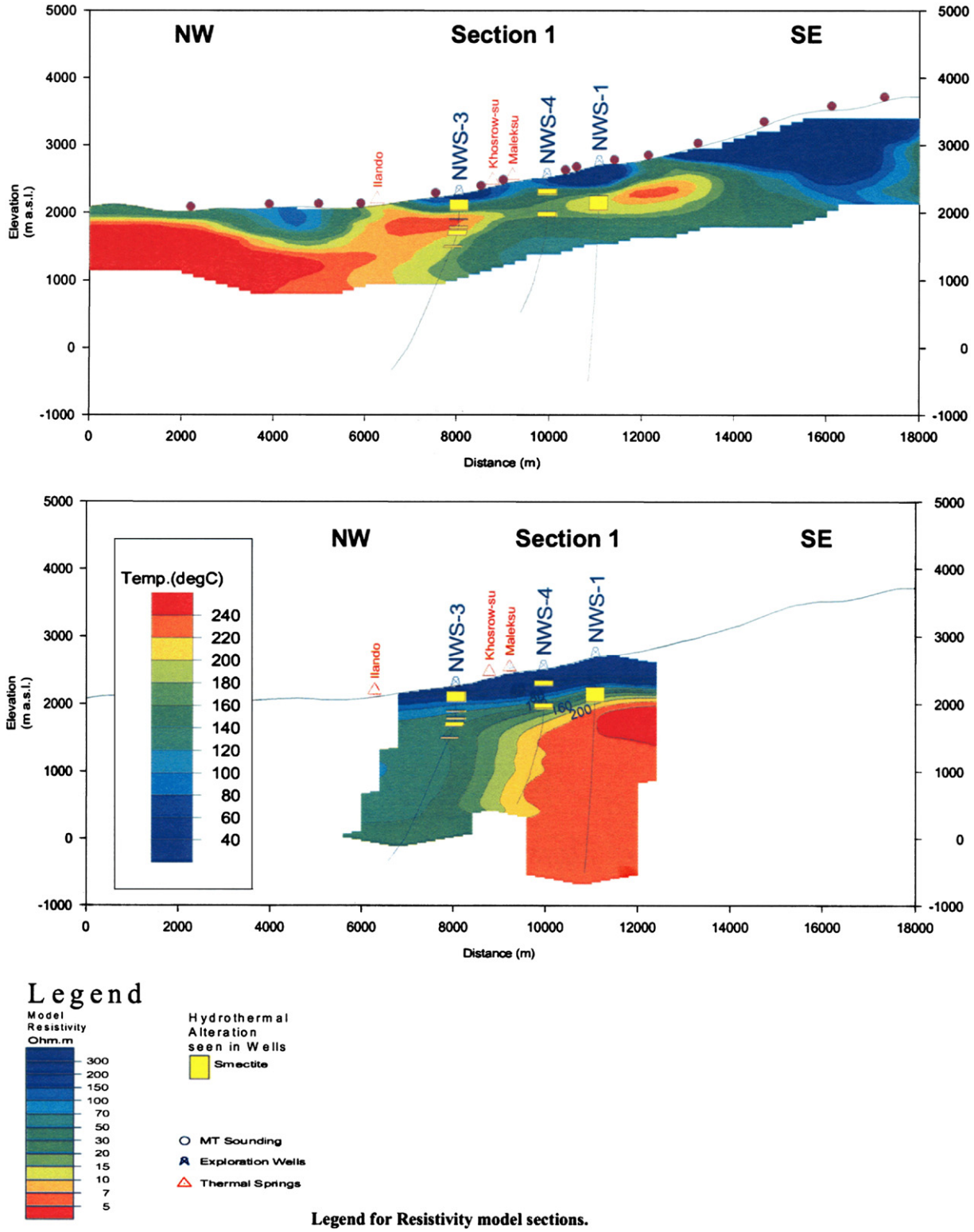

Fig. 7. 2-D resistivity section along the profile 1 (top) and corresponding temperature distribution (bottom) revealed from exploration wells (after Talebi et al., 2005).

and reduce drilling costs. Svetov (2006) has recently shown that seismoelectric (SE) transfer functions calculated from the EM data, measured at the earth's surface or in the borehole, could be sensitive to the porosity and permeability of the earth's crust. Fig. 6 shows frequency characteristics of real and imaginary parts of SE transfer function (normalized by resistivity of a homogeneous crust) calculated for a longitudinal wave. The real part is additionally normalized by ω^2, and the imaginary by ω^3 (where ω is the EM field frequency). At not very high frequencies (Rek>0) the real part is proportional to porosity and is practically permeability independent (Fig. 6a), whereas the imaginary part depends only weakly on porosity and is proportional to permeability (Fig. 6b). These results give the impetus to further examine a methodology in the near future to estimate porosity and permeability based on SE data.

4.3. Alteration mineralogy

Alteration minerals produce comparable or even greater reductions in resistivity with respect to fluid flow. Resistivity distribution provides a clear indication of the presence of hydrothermal alteration minerals, and is often considered as an important tool to locate geothermal reservoirs. However, it is difficult to directly determine the alteration mineralogy from EM sounding data, since different mineral assemblages may show the same resistivity.

On the other hand, the temperature dependence of the alteration mineralogy makes it possible to interpret the resistivity layering in terms of temperature, provided the temperature is in equilibrium with the dominant alteration (Árnason et al., 2000). According to these authors, the upper boundary of the low resistivity cap corresponds to temperatures in the range of 50–100 °C, depending on the intensity of the alteration. The transition from the low resistivity cap to the resistive core corresponds to temperatures in the range of 230–250 °C. Thus, if alteration is in equilibrium with temperature, the mapping of the resistivity structure is in fact the mapping of isotherms.

Anderson et al. (2000) proposed simple imaging of the high-temperature geothermal reservoirs by mapping the base of the conductive layer on the assumption that it corresponds to the 180 °C isotherm. However, resistivity reflects the alteration but not the present temperature, if cooling has recently taken place. In this case resistivity should be considered as a maximum geothermometer

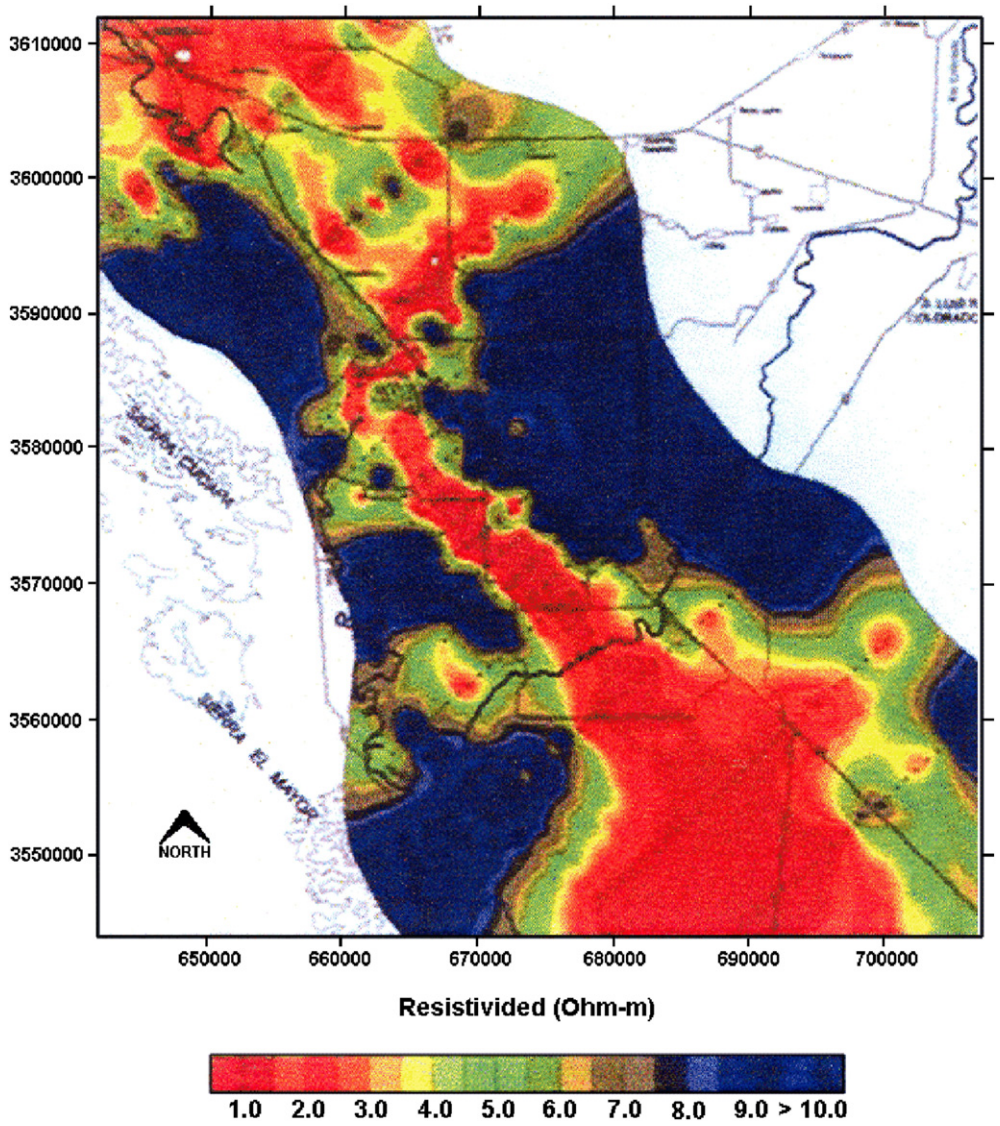

Fig. 8. Horizontal slice of the 3-D resistivity model obtained at 1200 m depth. Three linear trends seem to be present, two of them correspond to Cerro Prieto and Imperial faults (after Pérez-Flores et al., 2005).

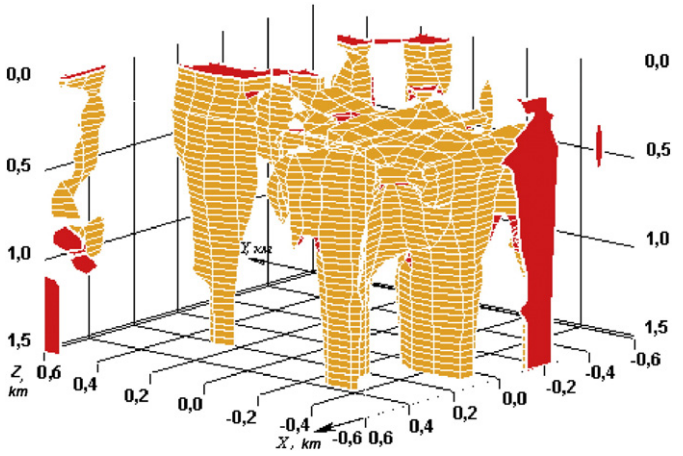

Fig. 9. Highly conductive cap (resistivity less than 6 Ω m) in the Minamikayabe geothermal zone (after Spichak, 2002).

(Árnason et al., 2000). In order to detect whether the geothermal system is still active, resistivity data should be supplemented by temperature data.

5. EM imaging geoelectric structure

5.1. Magnetotelluric studies

Of the various EM methods, magnetotelluric (MT) was found to be the most effective in defining a conductive reservoir overlain by a larger and more conductive clay cap. This is because the main anomaly related to the reservoir is caused by the presence of electric charges at conductivity boundaries rather than electromagnetic induction, and methods measuring also the electric field are superior to techniques that only employ magnetic field measurements (Pellerin et al., 1996). The depth of investigation of MT will be much greater at long source periods compared to most controlled-source EM methods. Such methods (see Section 5.2 on Other methods) are usually unable to detect geothermal reservoirs deeper than 1–2 km. The natural-field MT method has also proved very useful for mapping near-surface low resistivity zones caused by rock alteration and saline pore fluids in geothermal areas (e.g., Hoover et al., 1976, 1978; Long and Kaufman, 1980; Ushijima et al., 1986; Haak et al., 1989; Ingham, 1991; Anderson et al., 1995; Uchida, 1995; Lagios et al., 1998; Mulyadi, 2000; Uchida et al., 2000; Bai et al., 2001; Hafizi et al., 2002; Caglar et al., 2005; Correia and Safanda, 2002; Risk et al., 2002; Pérez-Flores and Schultz, 2002; Wannamaker et al., 2002, 2005; Volpi et al., 2003; Ushijima et al., 2005).

Since geology in geothermal areas is usually complex, a careful design of the MT survey is crucial. In Manzella (2004) the distance between MT sites was found to be of critical importance for defining the extension of low resistivity areas possibly associated to geothermal targets. As evidenced in the same paper, an anomalous low resistivity can be found also in geothermal areas where the main phase of the geothermal fluid is vapour circulating in crystalline rocks. This is possibly due to a fluid-phase in secondary fracture systems. The presence of geothermal fluids may also trigger dispersion phenomena over the frequency-dependent MT sounding data; however, when many electrical sounding data are available, and comparison of the high-frequency MT data and the electrical data defining the shallower structures gives an idea of the dispersion rate, this problem may be overcome (Manzella, 2004).

MT data inversion using geological and geophysical constraints enables not only to determine the general conductivity distribution in the studied area but also to delineate the geothermal reservoir and detect the cap layer. In particular, Uchida (1995) inverted the MT data in the Sumikawa geothermal field of northeastern Japan and interpreted a two-dimensional (2-D) resistivity model using drilling constraints such as temperature, porosity, clay mineral content and resistivity logs. The resulting resistivity model has two major features: 1) a cap layer of low resistivity (1–3 Ω m) due to low temperature clay minerals, and 2) a more resistive reservoir (~100 Ω m) in spite of its high temperature.

MT sounding enables also to indicate the location of permeable and fluid-saturated areas. In particular, Caglar et al. (2005) presented an MT survey in the Afyon part of the Taride zone in southwest Anatolia. Models of geoelectric structures obtained from 2-D inversion of MT

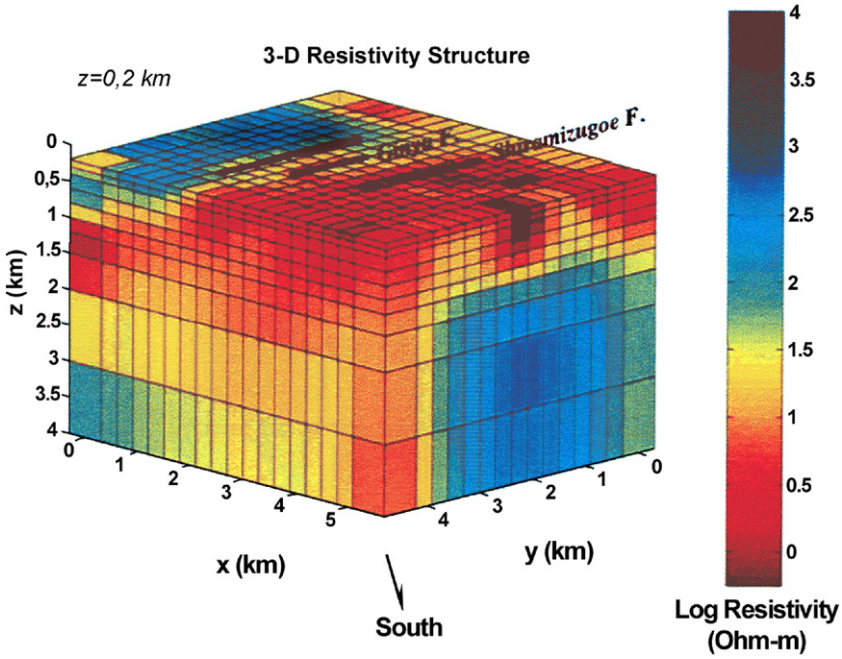

Fig. 10. 3-D view of the resistivity model of the Ogiri geothermal zone, Japan, from south. Shallow blocks to a 200 m depth are stripped out and approximate locations of three faults are overlaid (after Uchida, 2005).

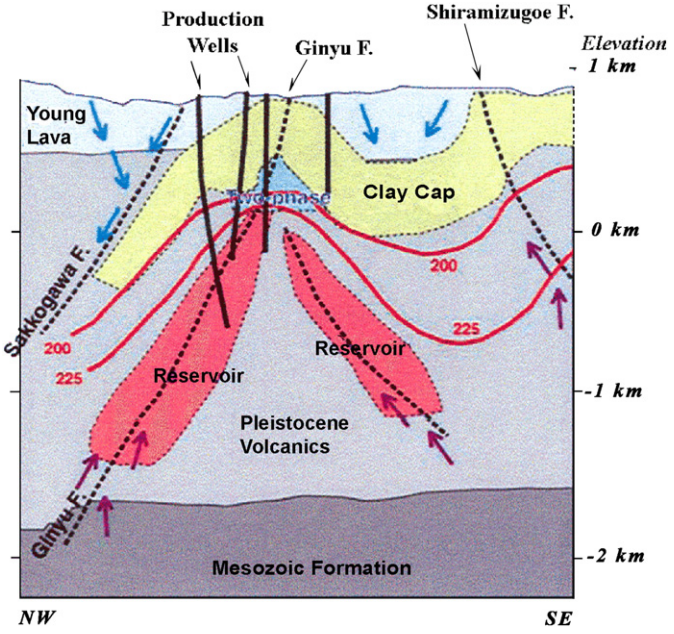

Fig. 11. A simplified geology section of the Ogiri geothermal zone along a NE–SW line around Lines A and B (reproduced from NEDO (2000)). Thick solid lines are several pilot and production wells. Red contours with numbers are temperature with values in °C. Thick black dashed lines indicate faults; thin dashed lines are estimated outlines of the reservoirs and clay cap. Arrows indicate estimated cold and hot water flows. (After Uchida, 2005.).

data clearly showed the existence of an electrically conductive (<50 Ω m) zone beneath the Sandikli graben geothermal region. Another conductive zone with resistivity values of 5–10 Ω m was defined beneath the seismically active Dinar graben. The authors believe that the very low resistivity values probably suggest that both zones are highly permeable and saturated with geothermal fluids.

MT soundings of volcanic geothermal areas enable to detect the location of the geothermal reservoir beneath the volcanic sediments (e.g., Ander et al., 1984; Eysteinsson and Hermance, 1985; Flóvenz et al., 1985; Hermance, 1985; Bartel and Jacobson, 1987; Mogi and Nakama, 1993; Bai et al., 2001; Talebi et al., 2005; Ushijima et al., 2005; Spichak et al., 2007b, etc.). In particular, Ushijima et al. (2005) used MT sounding to reveal anomalously low resistivity zones in the Takigami geothermal area, Kyushu, Japan, indicating a potential geothermal reservoir beneath the volcanic area. The low resistivity patterns often correlate with the distribution of smectite clay alteration products and are generally consistent with higher temperatures revealed from exploration wells (Talebi et al., 2005) (Fig. 7).

Thus, MT imaging of geothermal zones provides information on the base of the conductive clay cap and spatial location of the anomalously low resistivity zones which could be considered as candidates for being the geothermal reservoir. A comparison of the resistivity section with temperature distribution and alteration mineralogy enhances the reliability of MT data interpretation in geothermal terms.

5.2. Other methods

In areas where the geothermal circulation and related alteration take place at shallow depths (<1 km) it is better to use TEM or direct current (DC) methods. Bibby et al. (1995), Árnason et al. (2000) and Pérez-Flores et al. (2005) used DC (Schlumberger) sounding of the geothermal areas located in the Taupo volcanic zone (TVZ) of New Zealand, Iceland, and the Cerro Prieto region of Mexico, respectively, while Pérez-Flores and Gomez-Treviño (1997) applied DC (dipole–dipole) resistivity imaging of the Ahuachapan–Chipilapa (El Salvador) geothermal field.

In particular, the Cerro Prieto region was prospected with more than 400 long offset Schlumberger soundings. The geothermal area is at the center of a system of echelon faults that produce a slimming and possible rupture of the earth's crust. With the help of resistivity data, the authors obtained a 3-D resistivity image of the geothermal area and of the two principal faults that control the regional tectonics (Fig. 8). The application of fast imaging techniques developed by Pérez-Flores and Gomez-Treviño (1997) to dipole–dipole resistivity data in the Ahuachapan–Chipilapa area resulted in resistivity images that correlate with surface hydrothermal manifestations, information derived from drilled wells, and the results of MT surveys.

Árnason et al. (2000), Flóvenz and Karlsdottir (2000) and Demissie (2005) have reported on TEM soundings in Iceland. In the Eyjafjordur geothermal zone (northern Iceland), TEM resistivity soundings have been used by Flóvenz and Karlsdottir (2000) to create a resistivity image of the basaltic pile in the area to improve the older resistivity picture obtained by Schlumberger soundings. Inversion of the TEM soundings resulted in a layered resistivity model consisting of several layers of high and low resistivity with a southerly dip. This pattern had not been

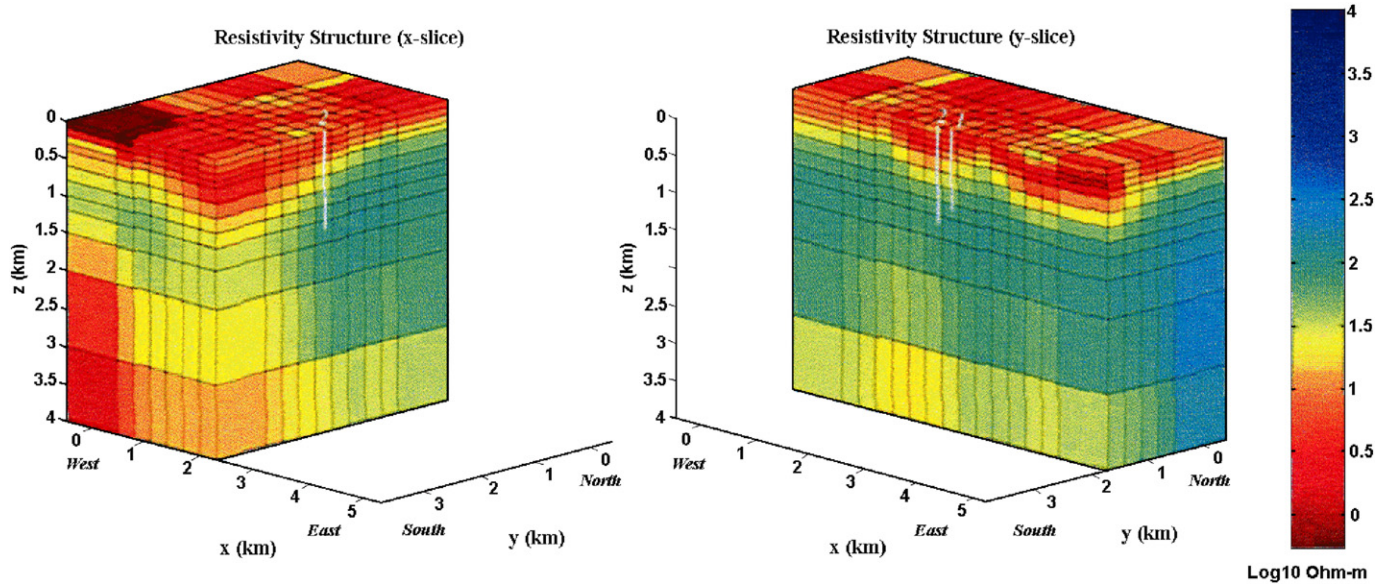

Fig. 12. 3-D view of the resistivity model of the Pohang low-enthalpy geothermal area, Korea. The volume is cut at an *x*-plane ($x = 2.25$ km) (left panel) and a *y*-plane ($y = 1.65$ km) (right panel). White bars indicate pilot drillings. (After Uchida et al., 2005.).

resolved in the previous Schlumberger soundings. A comparison of the TEM result with borehole and surface data shows that the resistivity layering coincides with the lithological one.

TEM sounding of geothermal areas has the following advantages over conventional DC surveys (Demissie, 2005):

- the transmitter couples inductively to the earth and no current has to be injected into the ground. In the places where the surface is dry and resistive this is of the utmost importance;
- the monitored signal is a decaying magnetic field rather than the electric field. This makes the TEM measurement much less dependent on local resistivity conditions at the receiver site. Distortion due to local resistivity non-uniformity at the receiver site can be a serious problem in DC measurements;
- with respect to the DC method, TEM is less sensitive to lateral resistivity changes;
- in DC sounding, the monitored signal is low when subsurface resistivity is low, as in geothermal areas, whereas in TEM soundings the situation is the reverse, the lower the resistivity the stronger the signal;
- central-loop TEM is more downward focused than the DC soundings. To increase the penetration depth in DC measurements, the electrode spacing and therefore the volume of rocks involved is increased, and the monitored electric field could be significantly affected. One-dimensional inversion is justified better in the interpretation of central-loop TEM sounding than in DC sounding;
- a TEM sounding requires less manpower than a DC Schlumberger sounding;
- with the instruments used in this survey, the DC soundings provide the best resolution in the uppermost 50–100 m, whereas for TEM soundings the resolution is better at greater depths.

Heat-triggering phenomena (such as thermoelectric and electrokinetic effects) due to hydrothermal circulation are manifested in self-potential (SP) anomalies observed at the earth's surface. Results obtained by Zlotnicki et al. (2006) show that SP anomalies could be an efficient indicator of the change in the thermal state and evolution of hydrothermal activity.

It is worth mentioning the method of resistivity and permittivity reconstruction from multi-frequency EM well-logging data proposed by Shen et al. (2000). It may improve the resolution of EM sounding in low resistivity contrast zones (especially in areas where the water injection technique is carried out).

5.3. 3-D models

The geological structure of geothermal areas is often very complicated due to hydrothermal circulation and alteration. Because of this, 1-D and 2-D interpretations of EM data may result in erroneous conclusions regarding the location and boundaries of the geothermal reservoir (especially in deep parts). Moreover, only 3-D models of the geothermal areas enable to guide the best locations for future drilling. 3-D modeling, imaging and inversion tools currently available enable to reconstruct the most adequate geoelectric structures of geothermal areas, which, in turn, could be used to estimate the volcano's energy (Mogi and Nakama, 1993), delineate the conductive clay cap (Spichak, 2002) (Fig. 9) and geothermal reservoirs (Yamane et al., 2000; Uchida, 2005; Uchida et al., 2005) (Figs. 10–12). By comparing the resistivity distributions with the temperature distributions based on fluid flow calculations at a steady state, the validity of the location and dimensions of the estimated reservoirs could be confirmed (Asaue et al., 2006).

Thus, the results discussed above clearly demonstrate the potential of the MT method in spatial mapping geothermal zones. 2-D interpretation of the MT data in such complicated areas as geothermal

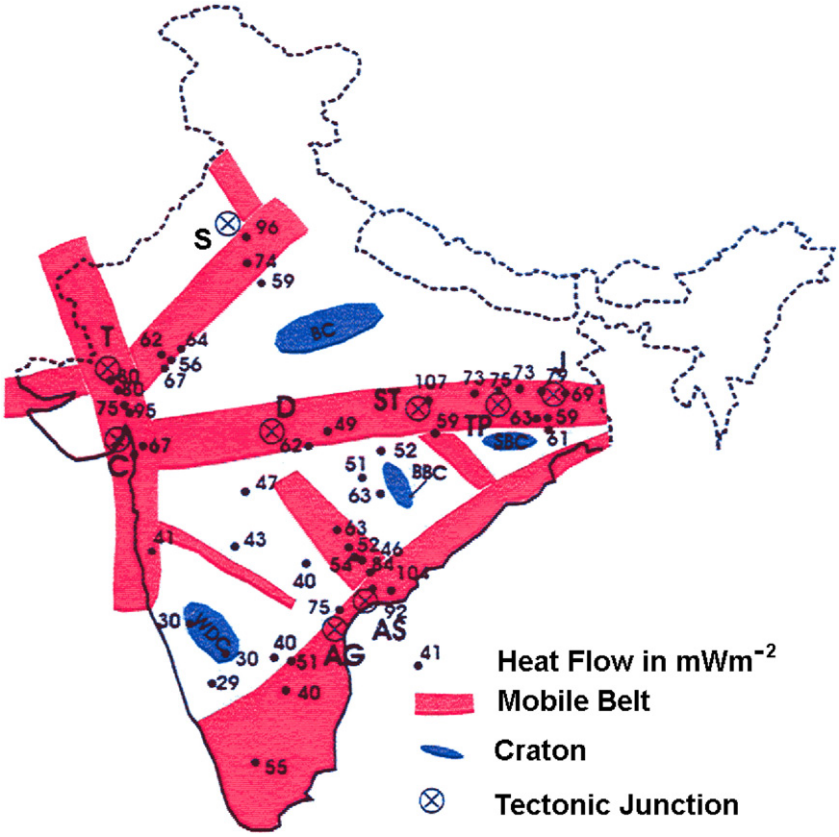

Fig. 13. Junctions of mobile belts and anomalous thermotectonics (circles with cross) along with the heat flow values in different regions of India. C: Cambay; TP: Tatapani, D: Damua/Parsia, J: Jharia, ST: Sonipat/Tusham, T: Tharad, AG: Agnigundala, AS: Aswaraopeta, etc. (after Veeraswamy and Harinarayana, 2006).

zones is often insufficient. Modern 3-D inversion methods provide appropriate tools for adequate resistivity reconstruction and, thus, for correct interpretation of the MT monitoring results, a more reliable estimation of the energetic potential of the reservoir and guiding locations for future drillings (see in this connection Sections 7 and 10, accordingly below).

6. Tectonics, faulting and fracturing

In terms of plate tectonics, geothermal regions occur mainly at or near divergent and convergent plate boundaries (spreading ridges and subduction zones), at intraplate rifts (continental rifts, and thermal anomalies (hot spots)). Plate movement may be accompanied by magma intrusions into the crust and by volcanism. Tectonic activity may cause deep faults and fractures in the sedimentary cover and in the upper crust. Fig. 13 shows junctions of mobile belts and anomalous thermotectonics (circles with cross) along with the heat flow values in different regions of India (Veeraswamy and Harinarayana, 2006). In these areas heat is transferred from the earth's interior not only by conduction but also by vertical mass transfer, such as upwelling of magma or deep water circulation and heat flow is often increased regionally with local extrema.

The presence of high conductive anomalies in the upper crust of the Himalayan belt region is attributed to the presence of partial melt generated from the subducted Indian crust. Harinarayana and Veeraswamy (Harinarayana et al., 2006; Veeraswamy and Harinarayana, 2006) studied the Puga and Tatapani geothermal zones, located in the tectonically active regions of India, using 2-D inversion of MT data. The subsurface sections along three E–W oriented profiles (Fig. 14) indicated the presence of an anomalous high-conductivity zone up to a depth of about 300–400 m near the center of the profile. Such an area is also evident at a depth of about 1.5 to 2 km. The deeper anomalous feature is clearly delineated with a width of about 4 km indicating its greater size, which probably represents the geothermal reservoir. Maybe, the most useful way to get an idea about local and regional tectonics which are related to the subduction and distensional processes is to provide analysis of azimuths of the major axes of the MT impedance ellipses and Parkinson induction arrows (Galanopoulus et al., 1991).

Rock fracturing is necessary for a promising reservoir and for the maintenance of well capacities throughout the life of the geothermal power plant. It leads to an increase in rock permeability, which, in turn, provides favorable conditions for hydrothermal fluid circulation. The latter is often detected along faults, thus EM sounding of faulted zones

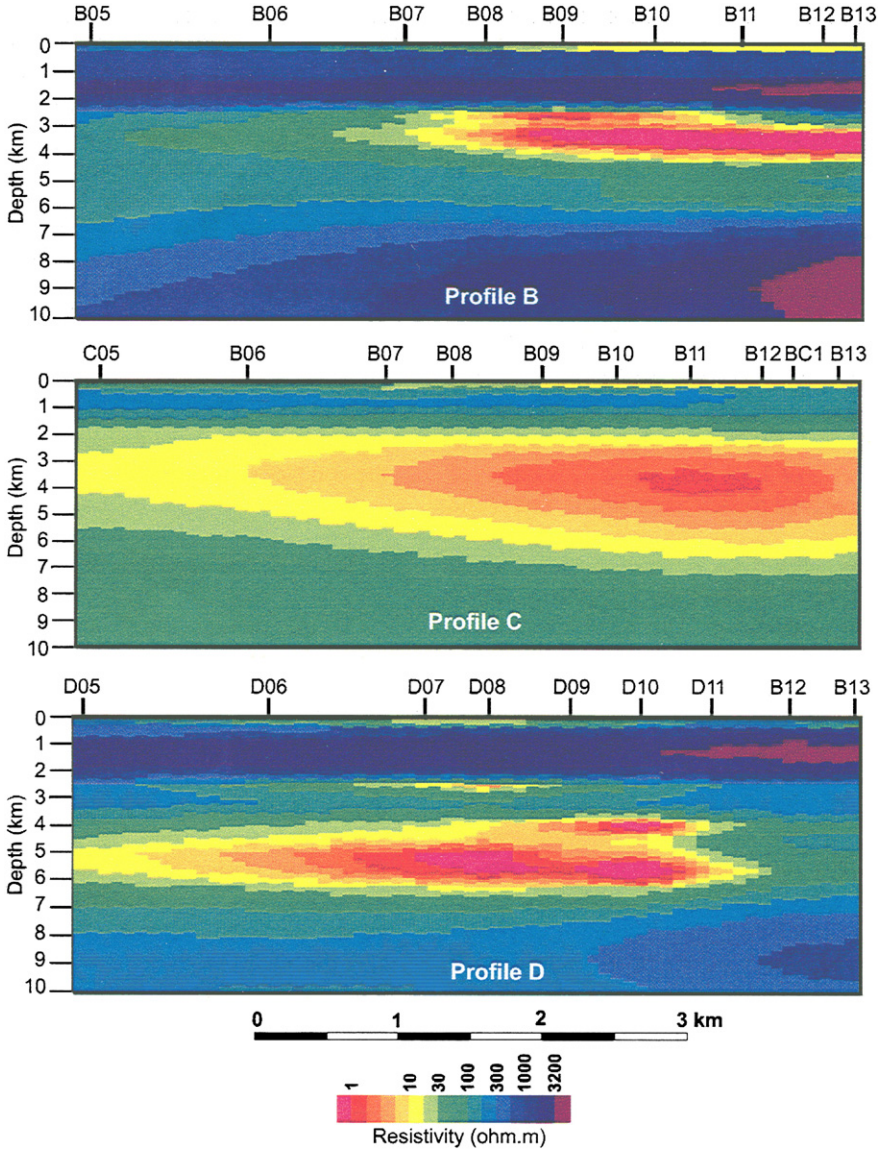

Fig. 14. Geoelectric cross-section obtained from the 2-D inversion of magnetotelluric data along three profile lines (B (top), C (middle) and D (bottom)) in the Puga geothermal area, India (after Harinarayana et al., 2006).

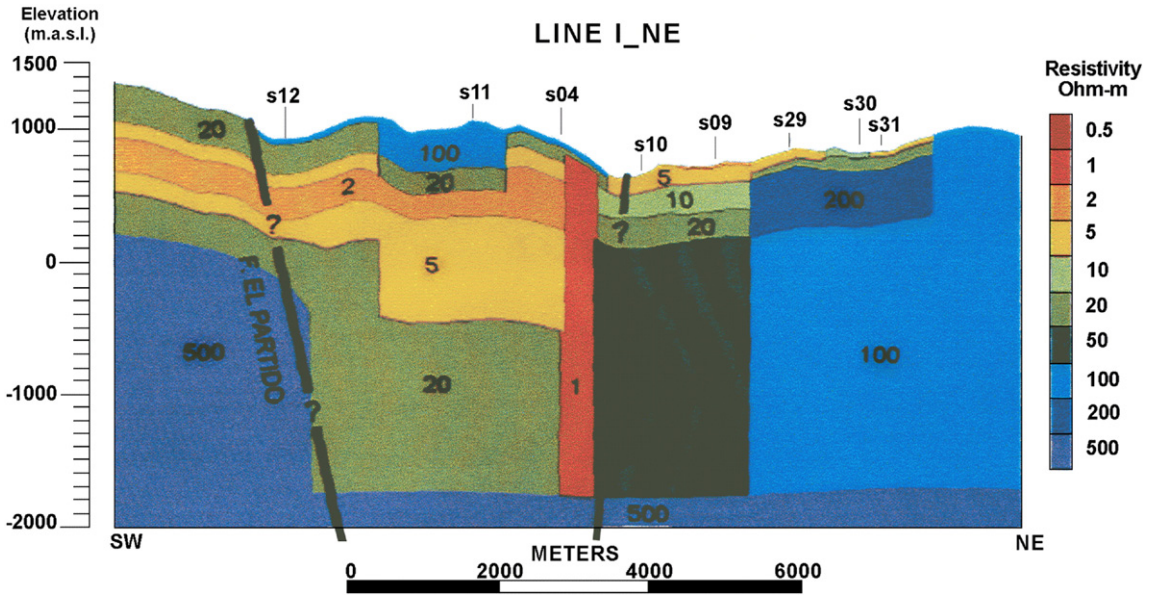

Fig. 15. Subsurface resistivity model of the Las Tres Virgenes geothermal field (Baya California Peninsula, Mexico) along line I_NE (after Romo et al., 2000).

may help to guide the location of geothermal reservoirs (e.g., Ushijima et al., 1986; Galanopoulus et al., 1991; Bromley, 1993; Bibby et al., 1995; Correia and Jones, 1997; Wannamaker, 1997a,b; Lagios et al., 1998; Romo et al., 2000; De Lugao et al., 2002; Wannamaker et al., 2002; Del Rosario et al., 2005; Layugan et al., 2005; Manzella et al., 2006).

Romo et al. (2000) used MT measurements at 90 sites to estimate the subsurface distribution of the electric conductivity at a depth range from 0 to 3 km. The results suggest the presence of a highly attenuating and conductive zone along the El Azufre Canyon (the boundary between Las Tres Virgenes complex and El Aguajito complex), which corresponds to the production interval of wells LV-2 and LV-3/4. A graben structure (Fig. 15), outlined between sites s12 and s10, is bounded by 1 Ω m vertical conductors presumably associated with the El Partido and El Azufre faults.

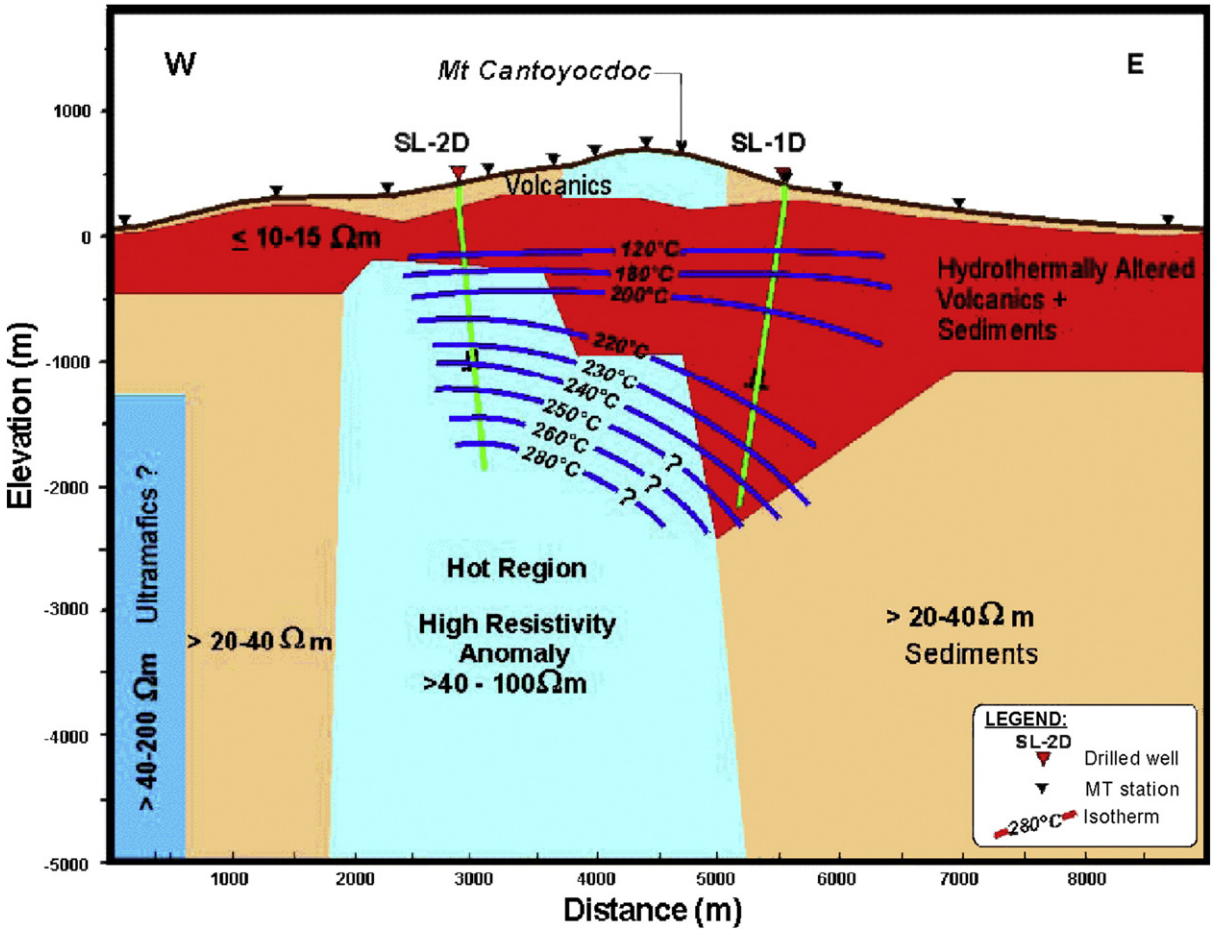

Fig. 16. MT resistivity structure correlated with lithology and temperature at Southern Leyte, Philippines (after Layugan et al., 2005).

In contrary to the above case the geothermal areas located in andesitic volcano-sedimentary systems (Layugan et al., 2005; Los Banos and Maneja, 2005) are often more resistive than surrounding sediments being caused by high-temperature but less conductive minerals such as illite, epidote, actinolite and garnet developed within the sediments. Fig. 16 shows the 2-D resistivity model of the Southern Leyte geothermal field (Philippines) as an example. The intrusion-like resistive body (>40–100 Ω m) beneath the western area of Mt. Cantoyocdoc is interpreted by the authors as the hottest region of the geothermal system. The high resistivity area is bounded by moderate resistivity values (>20–40 Ω m) that most likely reflect the sedimentary rock situated away from the center of the resource, where geothermal activity is absent.

Wannamaker (1997b) showed the advantages of having long period MT data combined with controlled-source audio-magnetotelluric (CSAMT) data when surveying the characteristics of the Sulphur Springs faulting thermal area in the U.S.A. Parameterized 2-D inversion of this data resulted in four geoelectric cross-sections indicating the main structural elements (Wannamaker (1997a) (Fig. 17). The low resistive zone detected in the Paleozoic sedimentary layer to the southwest of the Sulphur Creek Fault (SCF) appears to represent (although not necessarily) the hydrothermal aquifer, while the high resistivity area in the upper 500 m near wells VC-2B and VC-2A possibly corresponds to a vapor zone.

It is worth mentioning that in spite of the resistivity anomalies are controlled mainly by faulted structures, the resistivity variations not necessarily reflect the formational boundary nor the lithological differences of the rocks mapped in the area. Del Rosario et al. (2005) used the lithologics penetrated by the nearby wells to show the geothermal implication of the resistivity results. The authors categorized the Malabuyoc geothermal system as a basement aquifer beneath a sedimentary basin with the heated fluid originating east of the survey area. The fluid is channeled along the Middle Diagonal and Montaneza River Faults (MRF) and emerged along the stretch of the Montaneza River as warm seepages. Fig. 18 shows the geophysical model of the Malabuyoc thermal system at 250 m below sea level.

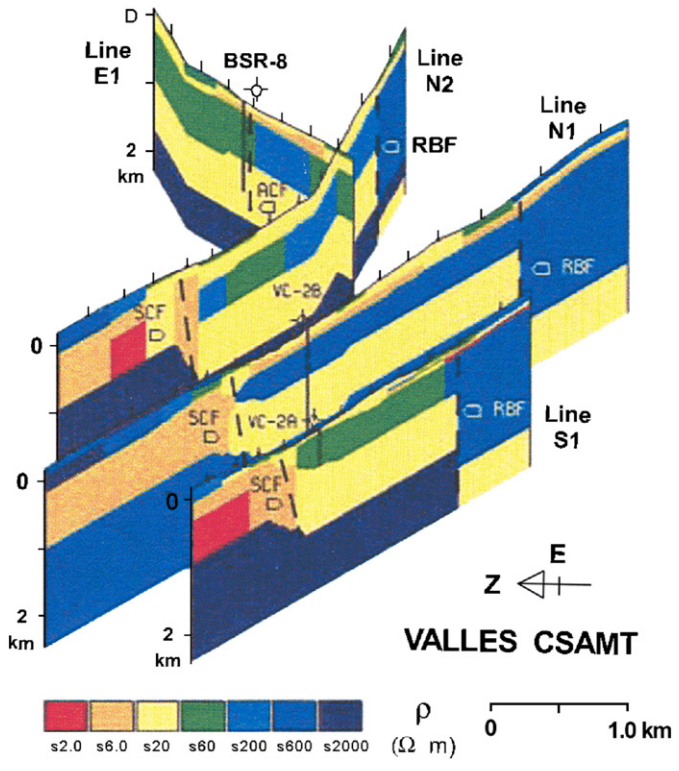

Fig. 17. Fence diagram assembling best-fit 2-D resistivity models for the Sulphur Springs area, USA. The models are vertically compressed by a factor of two for visibility. Details of the finite-element mesh geometry have been preserved, but resistivities have been grouped into half-decade intervals for simplicity. Surface locations of boreholes are plotted and projected upon the nearest resistivity section. Locations on each section of the Sulphur Creek Fault (SCF), Redondo Border Fault (RBF), and Alamo Canyon Fault (ACF) are noted (after Wannamaker, 1997a).

Another problem associated with finding the fluid circulation zones by EM methods is that the correlation between low resistivity and fluid concentration is not always correct since alteration minerals produce comparable and often a greater reduction in resistivity. Moreover, although water-dominated geothermal systems have an associated low resistivity signature, the opposite is not true. Low resistivity anomalies are not always suitable as geothermal targets; however, if they are accompanied by low-density anomalies this may increase the probability of such a conclusion. Therefore, integration with geological, other geophysical and drilling data can help to distinguish low resistivity geothermal targets from those related to different geological conditions.

Thus, EM sounding of tectonically active areas enables to detect faulted and fractured zones, which, in turn, often indicate the possible location of the hydrothermal circulation.

7. EM monitoring

Phase change of pore fluid (boiling/condensing) in fractured rocks can result in resistivity changes that are more than one order of magnitude greater than those measured in intact rocks. Secondly, production-induced changes in resistivity can provide valuable insights into the evolution of the host rock and resident fluids. Therefore, EM monitoring of the faults' macro-parameters may provide important information about their activity and fluid content.

Spichak and Popova (2000) developed an artificial neural network (ANN) expert system for the interpretation of MT monitoring of the fault macro-parameters. The authors concluded that the ability of ANN to teach itself by real geophysical (not only electromagnetic) data measured at a given location over a sufficiently long period means that the potential exists for using this approach to interpret monitoring data in different geological environments providing that prior knowledge about their resistivity structure is available (in particular, from MT sounding).

The impedance determinant is one of the most suitable data transforms for an adequate interpretation of MT measurements carried out with the aim of monitoring resistivity variations in the geothermal reservoir (Spichak, 2001). The author also showed by means of 3-D numerical modeling that the conductive channel (for instance, a fluid-filled fault or a chain of hot springs) connecting the reservoir with the surface strengthens the effect of the variation in the resistivity inside the reservoir. Firstly, it increases the diameter of the zone to enable reliable monitoring, and secondly it reduces the period threshold sufficient for the detection of even small variations in electrical resistivity.

At first glance, the construction of a 3-D geoelectric model of the zone under study and also the monitoring of crucial parameters would seem to require synchronous measurements carried out at MT sites regularly distributed over the earth's surface. However, forward numerical modeling indicates (Spichak, 2001) that restricting the monitoring to just the electric conductivity alteration inside the local area in the earth (for instance, a geothermal reservoir or magma chamber) may be sufficient for a proper interpretation of the data regularly measured even at one site at the surface. Since very few 3-D MT surveys and little interpretation experience is available in the world, only the above-mentioned computer simulation both of the MT fields' behavior and of the monitoring process itself may provide an appropriate basis for effective 3-D MT imaging and monitoring of geothermal zones.

The correct interpretation of the MT monitoring results depends to a great extent on the knowledge about the 3-D resistivity structure of the zone considered. Many seismic and EM studies are carried out aimed at determining “final” three-dimensional models of the regions. It may be that the best way to achieve this goal is to carry out synchronous measurements of MT data at the sites regularly distributed over the

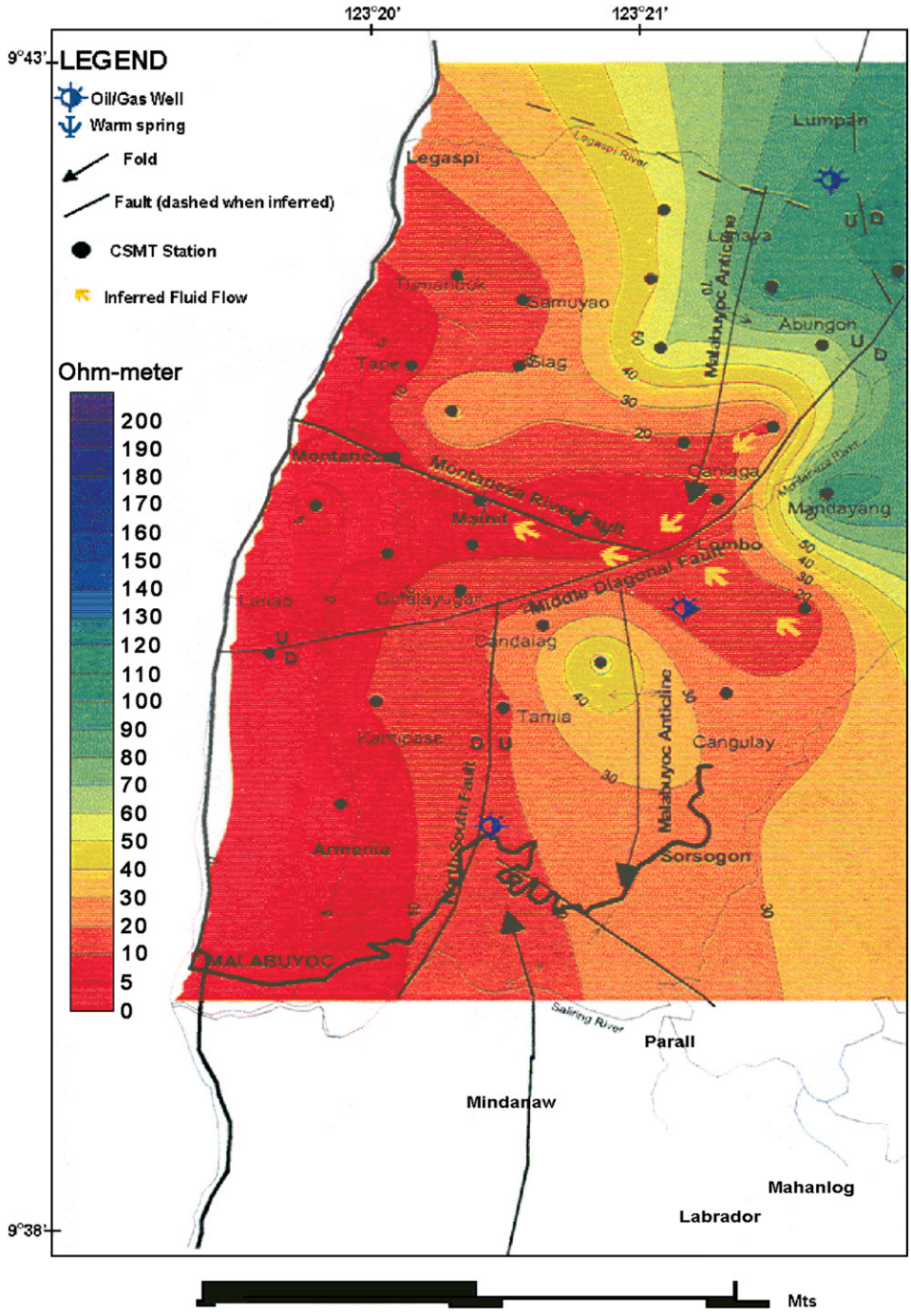

Fig. 18. Geophysical model of the Malabuyoc thermal system, Philippines, at 250 m below sea level (after Del Rosario et al., 2005).

surface. However, such an experiment would result at best in a construction of quite a good 3-D resistivity model that might change unpredictably before the next monitoring measurements are carried out. Thus, the interpretation of the results based on an already inadequate model would lead to an inaccurate estimation of the parameters monitored.

Thus, it is important to use a methodology that will closely link the monitoring results with knowledge about the internal structure at the moment of the last measurements. In other words, it should enable, on the one hand, the 3-D resistivity model of the studied zone to be updated in accordance with the new MT data collected at it's surface or surrounding area. On the other hand, it should take into account the current 3-D resistivity structure of this zone when interpreting the monitoring results.

Another problem concerns the methodology of the MT survey. The positions of sites as well as the survey regime depend on the aim of the MT sounding. Meanwhile, it would be very tempting to be able to use the results of any MT measurements carried out over the surface both to improve one's knowledge of the 3-D interior and for monitoring purposes. Thus, the problems of effective MT surveying, imaging and monitoring geothermal zones are threefold and need solving in close relation to each other.

8. Noise effect

Cultural noise could greatly contaminate the results of MT soundings. Uchida et al. (2005) observed very strong artificial noise at a frequency band of 0.1 Hz to 100 Hz at the survey area in Korea, which was interpreted

as being due to leakage currents from power line systems. Extremely coherent noise produced by the currents discharged by the direct current electrified railways at the passage of trains was found to be pervasive in the period range of 1–0.001 Hz and required considerable study and data processing (Larsen et al., 1996). However, use of remote-reference analysis with a remote station meant that most of these noises could be removed. Experience thought that it is not sufficient to use a reference site that appears to give good plane-wave results locally, since there may be EM noise fields (albeit planar) that correlate with those of the survey area. A combination of local and far remote sites, to face both local high-frequency noise and far, planar noise sources, proved to be the most effective solution (Larsen et al., 1996; Wannamaker et al., 2005; Manzella et al., 2006).

In relation to this, it is worth mentioning a paradoxical way of solving the noise problem suggested by Spichak et al. (1999a) for ANN interpretation of MT data. The authors found that prior mixing of the synthetic teaching data with an artificial noise may result in a significant reduction in ANN recognition errors (up to 5–10%) even if the noise level in the data reaches 50%. A number of approaches are currently used to reduce the negative effect of cultural noise. A complete review is out of the scope of this paper, however, the most recent trends in MT data processing and analysis can be found in Varentsov (2006).

Accurate interpretation of magnetotelluric data in the presence of static shift arising from near-surface inhomogeneities (geological noise) is still an open issue. It is common practice to correct the near-surface resistivity values with results of DC and/or TEM surveys (Ushijima et al., 1986; Bromley, 1993; Gunderson et al., 2000; Romo et al., 2000; Kajiwara et al., 2000; etc.). In order to reduce the negative effect of the static shift on the results of MT soundings Spichak (2001) proposed a technique based on the upward analytical continuation of the anomalous MT field at

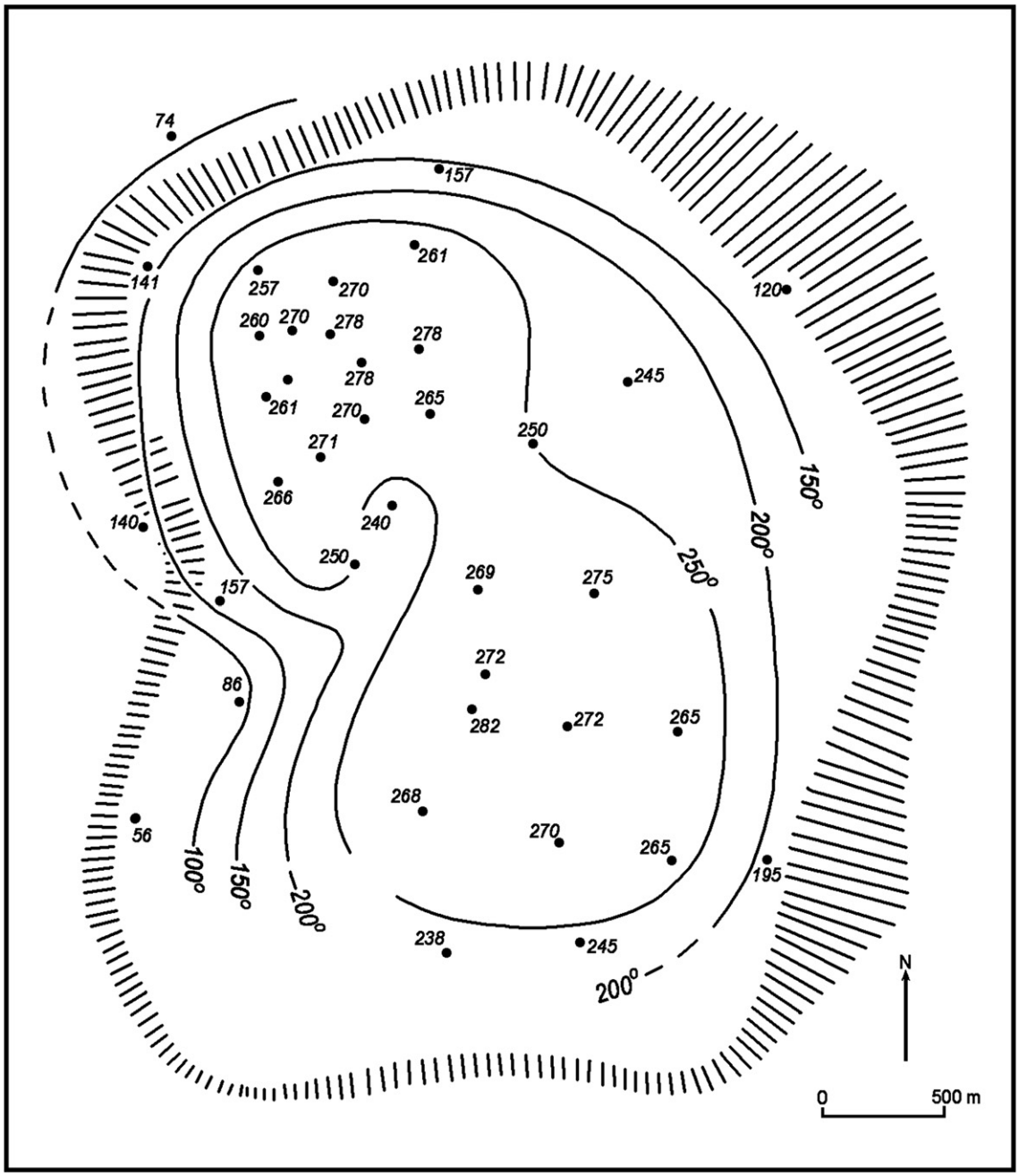

Fig. 19. Correlation of the boundary zone of Broadlands Geothermal Field, determined from resistivity measurements (hatched zone), with temperatures measured in drillholes in the geothermal field. Temperature data are seldom available from outside the boundary zone (after Bibby et al., 1995).

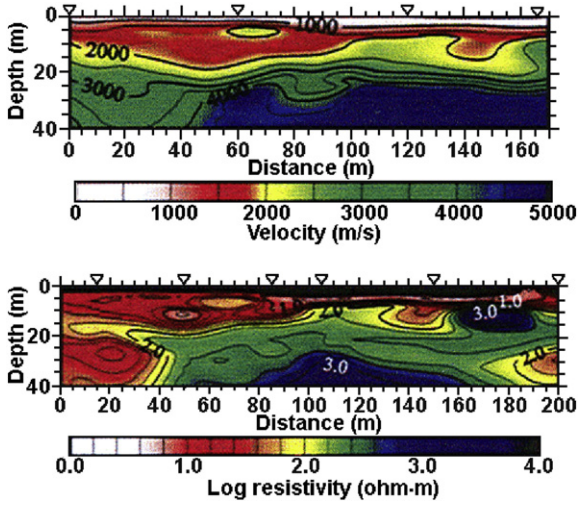

Fig. 20. Optimal 2-D joint velocity (top) and resistivity (bottom) models of the area composed from highly fractured granodiorite rock-mass (after Gallardo and Meju, 2003).

the reference plane located 200–500 m higher than the top topographic point by means of integral transformations. The use of the upward analytical continuation of MT data at the artificial reference plane allows not only the data that is necessary for appropriate further imaging to be filtered, but also to be reduced to a "common denominator" if they are collected over the relief surface, which often happens in volcanic environments. Another way could be based on joint inversion for magnetotelluric resistivity and static shift distributions (Sasaki and Meju, 2006), which significantly reduces the artifacts caused by static shift and improves the overall resolution of unknown parameters.

Thus, despite the problem of the industrial and geological noise in the EM data is not yet solved, we can conclude that recent findings mentioned above may essentially decrease its negative effect on EM sounding results.

9. Use of geological and other geophysical data

In order to reduce the uncertainty of EM inversion results (especially when using 1-D or 2-D inversion schemes) it is often useful to add information that comes from geological or other geophysical methods. This can be accomplished in different ways, the most common being an interpretation of the posterior resistivity distribution taking into account geophysical constraints in terms of the temperature well records and gravity or seismic velocity maps (Galanopoulus et al., 1991; Takasugi et al., 1992; Bibby et al., 1995; Lagios and Apostolopoulos, 1995; Correia and Jones, 1997; Gunderson et al., 2000; Talebi et al., 2005; Ushijima et al., 2005; Harinarayana et al., 2006; Spichak et al., 2007b, etc.).

In addition to individual DC soundings, Bibby et al. (1995) used over 7000 gravity measurements, temperature and seismic refraction data. Gravity measurements indicated that to a depth of about 2.5 km the upper layers of the Taupo volcanic zone consist of low-density pyroclastic infill. A seismic refraction interface with a velocity change from 3.2 km/s to 5.5 km/s occurs at a similar depth. The cross-sectional area of the convection plumes (identified by DC sounding) appears to increase at depths of 1–2 km, consistent with a decrease in permeability at the depth at which the velocity and density increase. The authors found that the pattern of low resistivity anomalies detected by DC sounding data delineates the horizontal extent of the near-surface distribution of hot water. Its boundary correlates with the transition from high to low temperatures measured in the drillholes (Fig. 19).

The relationship between electric resistivity and temperature was the main motivation for the MT survey on the Alentejo Geothermal Anomaly (AGA), detected in Hercynian structures in southern Portugal in the area of the intersection of the Messejana fault and the Ferreira–Ficalho overthrust (Correia and Jones, 1997). The results of the survey are

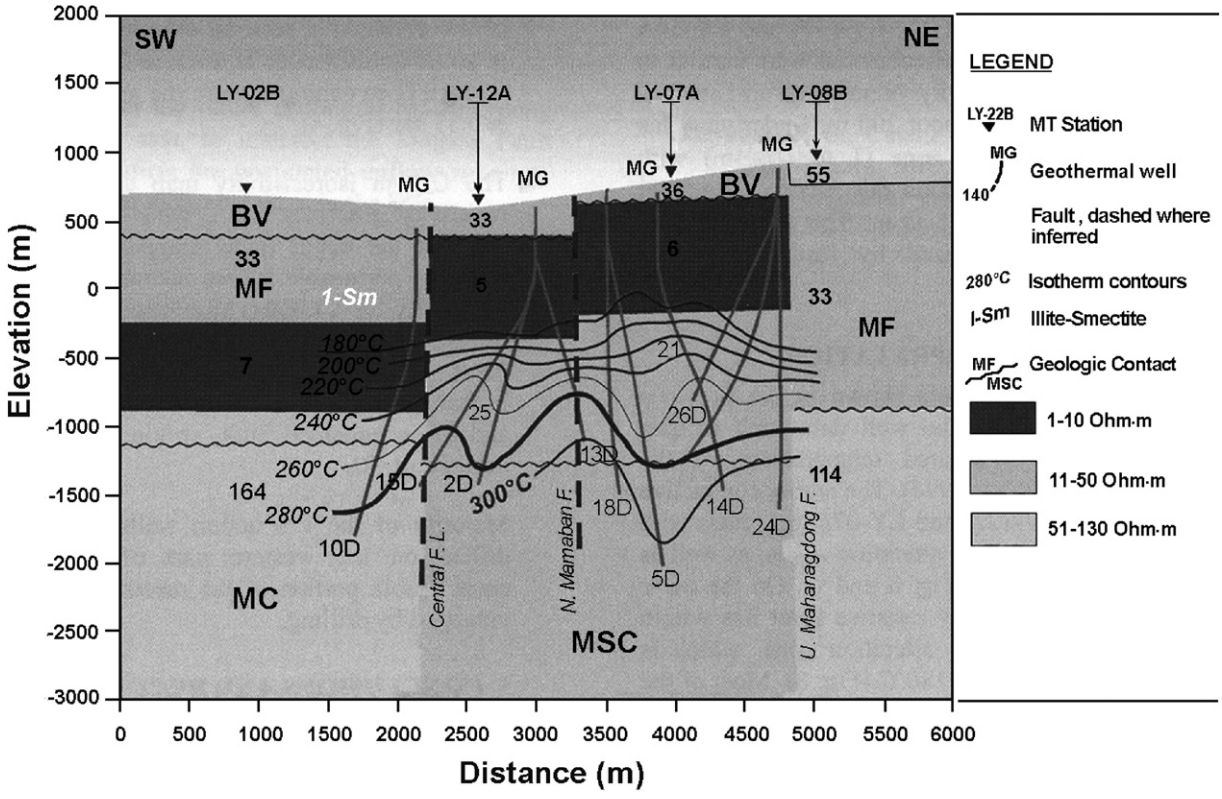

Fig. 21. Resistivity model along profile S-01 in the Mahanagdong geothermal field, Leite, Philippines (after Los Banos and Maneja, 2005).

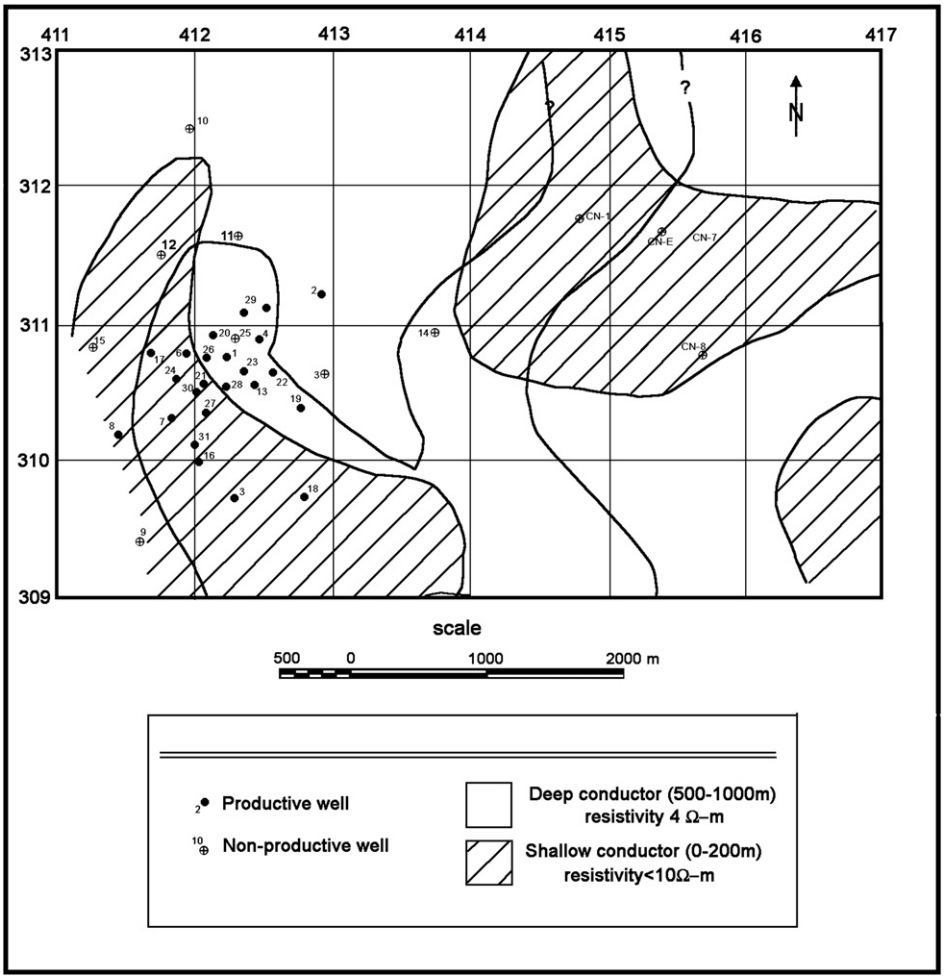

Fig. 22. Deep conductors and drillholes in the Ahuachapan–Chipilapa area (Romo et al., 1997).

discussed in conjunction with magnetic, gravimetric and seismic information as well as calculations of synthetic temperature distribution within the crust. The area studied appears to be a low electric resistivity region with a number of deeply rooted high electric resistivity blocks. The authors concluded that AGA is probably a shallow feature and does not represent the regional thermal regime of the crust in southern Portugal.

Finally, since the interface between the conductive cap (clay alteration halo) and the relatively resistive reservoir is largely controlled by the smectite distribution over the geothermal reservoir Gunderson et al. (2000) suggest refining the results of MT inversion by measuring the smectite contents in the wells.

A set of joint geological/geophysical data analysis/interpretation techniques is presently available. Application of these techniques to the EM and other data measured in the geothermal areas may increase the accuracy of the inversion schemes and result in more robust detection of the reservoir's macro-parameters. In particular, Gallardo and Meju (2003, 2007) developed a robust 2-D joint inversion scheme incorporating the concept of cross-gradients of electric resistivity and seismic velocity as constraints so as to investigate the resistivity–velocity relationships in complex near-surface environments more precisely. The results of their joint inversion of DC resistivity and seismic refraction data (Fig. 20) for the area consisting of a highly fractured granodiorite rock-mass suggest that it is possible to distinguish between different types or facies of unconsolidated and consolidated materials. This refines a previously proposed resistivity–velocity interrelationship derived from separate inversions of the respective data sets.

Another approach based on the post-inversion joint analysis of different properties was proposed by Spichak et al. (2006). The authors use to this end the method of maximal correlation similitude, which enables to find spatial clusters characterized by maximal correlation between different petrophysical parameters. It was recently used to construct the 3-D resistivity model of the Elbrus volcanic center (northern Caucasus) based on MT sounding data and maps of tectonic rock fragmentation that were revealed by the lineament pattern analysis (Spichak et al., 2007a).

It is important to be able to include the geophysical constraints in the interpretation procedure so as to avoid the unnecessary "personal" effect. Spichak et al. (1999b) proposed the 3-D inversion technique based on Bayesian statistics and Markov chains. The prior geological and geophysical information available is incorporated in the inversion procedure via the probability density function, specified for the prior resistivity palette in the region being investigated, while the parameters to be found are the posterior resistivity values. Posterior parameter uncertainties are also obtained, which are related to the amount and quality of both the input data and prior information.

10. Defining drilling targets

There are two points of view regarding the interpretation of the low resistivity zone defined in the geothermal area. One is that the low resistivity is a manifestation of the geothermal reservoir itself, which contains hot water in which there are dissolved chemicals. The other is that the low resistivity zone is regarded as a clay alteration halo

overlying the high-temperature reservoir. Accordingly, in the former, drilling targets are the low resistivity objects, whereas in the latter they are the moderately resistive layers underlying the very conductive ones. Therefore, the resistivity structure of the geothermal zone revealed by one of the EM methods should be considered as necessary but not sufficient information for making decisions regarding the drilling targets.

In the presence of the prior geological information about the type of the geothermal system it is possible to interpret the EM data in geothermal terms and accordingly to determine the drilling targets. In particular, Akiyoshi and Tagomori (2000) interpreted the geoelectric structure of the Hatchobaru geothermal field taking into consideration that most of geothermal reservoirs in the volcanic areas are of the fractured type and are controlled by the fault system. The authors used the mise-a-la-masse method, as well as MT and CSAMT, and were able to define the most promising zone for drilling, defined as the low resistivity areas where electrical discontinuities could be defined. Similarly, Mulyadi (2000) suggests that for future drilling permeable geological structures, such as faults in the resistive areas (45–75 Ω m) should be considered.

However, in the general case it is more reliable to supplement the resistivity data at least by the information from the wells. In particular, the delineated resistivity model shown in Fig. 21 (Los Banos and Maneja (2005) was correlated with well data such as clay alteration patterns and measured temperatures of the subsurface. The highly conductive middle layer beneath LY-12A and LY-07A coincides with smectite and smectite–illite alteration zones, as well as the 180 °C isotherm contour. On the other hand, the underlying moderately resistive layer lies within the illite, biotite and chlorite alteration zone, which is characterized by temperatures higher than 180 °C. Most of the production wells in this sector were drilled within this layer.

Correlation between the low resistivity and high-temperature zones leads to the conclusion that the influence of clay minerals resulting from hydrothermal alteration processes is not the main contributing factor to enhanced deep conductivities (Romo et al., 1997). The spatial distribution of the deep conductivity anomalies and of the productive wells in the Ahuachapan geothermal area (Fig. 22) suggests an interesting relationship: in 86% of the cases there is a positive correlation between the presence of a deep conductor and the occurrence of a productive well. This implies the existence of enhanced permeabilities, possibly the result of faulting and fracturing. This correlation, together with the temperature–conductivity relationship, suggest that the low resistivities found can be explained by the combined effect of high temperature and high permeability.

Therefore, decisions regarding drilling target depend on many factors (the main ones being information on the temperature, resistivity, permeability and alteration mineral distributions) and should be based on all the geological and geophysical information available in the geothermal area.

11. Conclusions

Thus, EM sounding of the geothermal zones enables

- to reveal stratigraphical layering;
- to produce a static image of the reservoir and surrounding structure;
- to locate fractures and faulted zones and determine the strike orientation;
- to detect the boundary between the cap formed by clay minerals and high-temperature reservoirs;
- to limit the uncertainties in the distribution of heat flow in the uppermost crust;
- to estimate the permeability values;
- to monitor the phase change of pore fluid in fractured rocks and resident fluids resulting in resistivity changes in the host rocks;
- to improve the accuracy of reservoir temperature estimates;
- finally, to reduce exploration costs.

EM sounding geothermal zones provides a useful contribution to geothermal exploration and exploitation through careful data acquisition, processing, modeling and interpretation. To take complete advantage of the potential of EM sounding of geothermal zones and distant monitoring macro-parameters of the reservoirs, fluid-filled faults and other elements of the geothermal system, it is important to use modern 3-D modeling and inversion techniques as well as EM data interpretation methodology quantitatively taking into account prior geological information and expert estimates and techniques that reduce the effects of industrial and geological noise.

Integration of EM data with rock physics data, lithology, temperatures, permeability, geological and other geophysical information will improve the imaging of static and dynamic processes in geothermal systems. The key element in the joint interpretation could be the use in geothermal reservoir simulators to obtain a conceptual model that complies with all the available data, both geophysical and thermohydraulic.

Acknowledgements

This study was performed within the Sixth EC Framework Programme (project ENGINE) and RBRF grant 07-05-00017. The authors acknowledge the anonymous referees for corrections and valuable suggestions that greatly improved the manuscript.

References

Akiyoshi, M., Tagomori, K., 2000. Geoelectrical structure of the Hatchobaru geothermal field and the adaptability of electrical methods for its understandings. Proc. World Geothermal Congress, Kyushu-Tohoku, Japan.
Ander, M.A., Gross, R., Strangway, D.W., 1984. A detailed magnetotelluric/audiomagnetotelluric study of the Jemez Volcanic Zone, New Mexico. J. Geophys. Res. 89 (B5), 3335–3353.
Anderson, E., Jacobo, E., Ussher, G., 1995. A geothermal reservoir revealed — magnetotelluric and data management techniques in a potent combination. Proc. World Geothermal Congress, Florence, Italy, pp. 899–902.
Anderson, E., Crosby, D., Ussher, G., 2000. Bulls-eye! — simple resistivity imaging to reliably locate the geothermal reservoir. Proc. World Geothermal Congress, Kyushu-Tohoku, Japan, pp. 909–914.
Archie, G.E., 1942. The electrical resistivity log as an aid in determining some reservoir characteristics. Trans. AIME 146, 54–67.
Árnason, K., Flóvenz, Ó.G., 1995. Geothermal exploration by TEM-soundings in central Asal Rift in Djibuti, east Africa. Proc. World Geothermal Congress, Florence, Italy, pp. 933–938.
Árnason, K., Haraldsson, G.I., Johnsen, G.V., Thorbergsson, G., Hersir, G.P., Saemundsson, K., Georgsson, L.S., Snorrason, S.P., 1986. Nesjavellir–Olkelduhalsr: A Geological and Geophysical Survey 1986. Orkustofnun Report OS-86018/JHD-02. 112 p. (in Icelandic).
Árnason, K., Karlsdottir, R., Eysteinsson, H., Flóvenz, O.G., Gudlaugsson, S.T., 2000. The Resistivity Structure of High-Temperature Geothermal Systems in Iceland, Geothermal Congress, Kyushu-Tohoku, Japan, pp. 923–928.
Asaue, H., Koike, K., Yoshinaga, T., Takakura, S., 2006. Magnetotelluric resistivity modeling for 3D characterization of geothermal reservoirs in the Western side of Mt. Aso, SW Japan. J. Appl. Geophys. 58 (4), 296–312.
Bai, D.H., Meju, M.A., Liao, Z.J., 2001. Magnetotelluric images of deep crustal structure of the Rehai geothermal field near Tengchong, southern China. Geophys. J. Int. 147, 677–687.
Bartel, L.C., Jacobson, R.D., 1987. Results of a controlled-source audio-frequency magnetotelluric survey at the Puhimau thermal area, Kilauea Volcano, Hawaii. Geophysics 52 (5), 665–677.
Berktold, A., 1983. Electromagnetic studies in geothermal regions. Geophys. Surv. 6, 173–200.
Bibby, H.M., Caldwell, T.G., Davey, F.J., Webb, T.H., 1995. Geophysical evidence on the structure of the Taupo Volcanic Zone and its hydrothermal circulation. J. Volcanol. Geotherm. Res. 68, 29–58.
Bromley, C., 1993. Tensor CSAMT study of the fault zone between Waikite and Te Kopia geothermal fields. J. Geomagn. Geoelectr. 45, 887–896.
Caglar, I., Tuncer, V., Kaypak, B., Avsar, U., 2005. A high conductive zone associated with a possible geothermal activity around Afyon, Northern Part of Tauride Zone, South West Anatolia. Proc. World Geothermal Congress, Antalya, Turkey.
Correia, A., Jones, F.W., 1997. On the existence of the geothermal anomaly in southern Portugal. Tectonophysics 271, 123–134.
Correia, A., Safanda, J., 2002. Geothermal modeling along a two-dimensional crustal profile in southern Portugal. J. Geodyn. 34, 47–61.
De Lugao, P.P., La Terra, E.F., Kriegshauser, B., Fontes, S.L., 2002. Magnetotelluric studies of the Caldas Novas geothermal reservoir, Brazil. J. Appl. Geophys. 49, 33–46.
Del Rosario Jr., R.A., Pastor, M.S., Malapitan, R.T., 2005. Controlled source magnetotelluric (CSMT) survey of Malabuyoc thermal prospect, Malabuyoc/Alegria, Cebu, Philippines. Proc. World Geothermal Congress, Antalya, Turkey.
Demissie, Y., 2005. Transient electromagnetic resistivity survey at the Geysir geothermal field South Iceland. Proceedings World Geothermal Congress, Antalya, Turkey.

Eysteinsson, H., Hermance, J.F., 1985. Magnetotelluric measurements across the eastern neovolcanic zone in south Iceland. J. Geophys. Res. 90, 10093–10103.
Flóvenz, O.G., Karlsdottir, R., 2000. TEM-resistivity image of a geothermal field in Iceland and the relation of the resistivity with lithology and temperature. Proc. World Geothermal Congress, Kyushu-Tohoku, Japan, pp. 1127–1132.
Flóvenz, O.G., Georgsson, L.S., Árnason, K., 1985. Resistivity structure of the upper crust in Iceland. J. Geophys. Res. 90, 10136–10150.
Flóvenz, O.G., Spangerberg, E., Kulenkampff, J., Árnason, K., Karlsdottir, R., Huenges, E., 2005. The role of electrical interface conduction in geothermal exploration. Proc. World Geothermal Congress, Antalya, Turkey.
Frischknecht, F.C., 1967. Fields about an oscillating magnetic dipole over a two-layered earth and application of ground and airborne surveys. Colo. Sch. Mines Q. 62, 1–326.
Fulignati, P., Malfitano, G., Sbrana, A., 1997. The Pantelleria caldera geothermal system; data from the hydrothermal minerals. J. Volcanol. Geotherm. Res. 75, 251–270.
Galanopoulus, D., Hutton, V.R.S., Dawes, G.J.K., 1991. The Milos geothermal field: modeling and interpretation of electromagnetic induction studies. Phys. Earth Planet. Inter. 66, 76–91.
Gallardo, L.A., Meju, M.A., 2003. Characterization of heterogeneous near-surface materials by joint 2D inversion of DC resistivity and seismic data. Geophys. Res. Lett. 30 (13), 1658.
Gallardo, L.A., Meju, M.A., 2007. Joint two-dimensional cross-gradient imaging of magnetotelluric and seismic travel-time data for structural and lithological classification. Geophys. J. Int. 169, 1261–1272.
Gianelli, G., Mekuria, N., Battaglia, S., Chersicla, A., Garofalo, P., Ruggieri, G., Manganelli, M., Gebregziabher, Z., 1998. Water–rock interaction and hydrothermal mineral equilibria in the Tendaho geothermal system. J. Volcanol. Geotherm. Res. 86, 253–276.
Gonzalez-Partida, E., Garcia Gutierrez, A., Torres Rodriguez, V., 1997. Thermal and petrologic study of the CH-A well from the Chipilapa–Ahuachapan geothermal area, El Salvador. Goethermics 26, 701–713.
Gonzalez-Partida, E., Birkle, P., Torres-Alavarado, I.S., 2000. Evolution of the hydrothermal system at Los Azufres, Mexico, based on petrologic, fluid inclusion and isotopic data. J. Volcanol. Geotherm. Res. 104, 277–296.
Gunderson, R., Cimiming, W., Astra, U., Harvey, C., 2000. Analysis of smectite clays in geothermal drill cuttings by the methylene blue method: for well site geothermometry and resistivity sounding correlation. Proc. World Geothermal Congr., Kyushu-Tohoku, Japan, pp. 1175–1181.
Haak, V., Ritter, O., Ritter, P., 1989. Mapping the geothermal anomaly on the island of Milos by magnetotellurics. Geothermics 18 (4), 533–546.
Hafizi, M.K., Aiobi, M., Rahimi, A., 2002. The combination of 2-D and 1-D inversion for 2.5D interpretation of magnetotelluric geothermal sites. Expanded abstr. EAGE 64th Conference, Florence, Italy.
Harinarayana, T., Abdul Azeez, K.K., Murthy, D.N., Veeraswamy, K., Eknath Rao, S.P., Manoj, C., Naganjaneyulu, K., 2006. Exploration of geothermal structure in Puga geothermal field, Ladakh Himalayas, India, by magnetotelluric studies. J. Appl. Geophys. 58 (4), 280–295.
Hermance, J.F., 1985. Magnetotelluric measurements across the Eastern neovolcanic zone in south Iceland. J. Geophys. Res. 90 (B12), 10093–10103.
Hoffmann-Rothe, A., Ritter, O., Haak, V., 2001. Magnetotelluric and geomagnetic modelling reveals zones of very high electrical conductivity in the upper crust of Central Java. Phys. Earth Planet. Inter. 124 (3–4), 131–151.
Hoover, D.B., Frischknecht, F.C., Tippens, C., 1976. Audiomagnetotelluric soundings as reconnaissance exploration technique in Long Valley, California. J. Geophys. Res. 81, 801–809.
Hoover, D.B., Long, C.L., Senterfit, R.M., 1978. Some results from audiomagnetotelluric investigations in geothermal areas. Geophysics 43, 1501–1514.
Ingham, M.R., 1991. Electrical conductivity structure of the Broadlands–Ohaaki geothermal field, New Zealand. Phys. Earth Planet. Inter. 66, 62–75.
Kajiwara, T., Mogi, T., Fomenko, E., Ehara, S., 2000. Three-dimensional modeling of geoelectrical structure based on MT and TDEM data in Mori geothermal held, Hokkaido, Japan. Proc. World Geothermal Congress, Kyushu-Tohoku, Japan, pp. 1313–1318.
Lackschewitz, K.S., Singer, A., Botz, R., Schonberg, G.D., Stoffers, P., Horz, K., 2000. Formation and transformation of clay minerals in the hydrothermal deposits of Middle Valley, Juan de Fuca Ridge, ODP Leg 169. Econ. Geol. 95, 361–389.
Lagios, E., Apostolopoulos, G., 1995. Integrated geophysical study of the geothermal system in the southern part of the Nisiros Island, Greece. J. Appl. Geophys. 34, 55–61.
Lagios, E., Galanopoulos, D., Hobbs, B.A., Dawes, G.J.K., 1998. Two-dimensional magnetotelluric modelling of the Kos Island geothermal region (Greece). Tectonophysics 287, 157–172.
Larsen, J.C., Mackie, R.L., Manzella, A., Fiordelisi, A., Rieven, S., 1996. Robust smooth magnetotelluric transfer functions. Geophys. J. Int. 124, 801–819.
Layugan, D.B., Rigor Jr., D.M., Apuada, N.A., Los Bafios, C.F., Olivar, R.E.R., 2005. Magnetotelluric (MT) resistivity surveys in vanous geothermal systems in Central Philippines. Proc. World Geothermal Congress, Antalya, Turkey.
Lebedev, E.B., Khitarov, N.I., 1964. Dependence of the beginning of melting of granite and electrical conductivity of its melt on high water vapor pressure. Geokhimija 195–201 (in Russian).
Long, C.L., Kaufman, H.E., 1980. Reconnaissance geophysics of a known geothermal resource area, Weiser, Idaho, and Vale, Oregon. Geophysics 45, 312–322.
Los Banos, C.F., Maneja, F.C., 2005. The Resistivity Structure of the Mahanagdong Geothermal Field, Leyte, Philippines. Proc. World Geothermal Congress, Antalya, Turkey.
Manzella, A., 2004. Resistivity and heterogeneity of Earth crust in an active tectonic region, southern Tuscany, Italy. Ann. Geophys. 47, 107–118.
Manzella, A., Spichak, V., Pushkarev, P., Sileva, D., Oskooi, B., Ruggieri, G., Sizov, Yu., 2006. Deep fluid circulation in the Travale geothermal area and its relation with tectonic structure investigated by a magnetotelluric survey. Expanded abstr. 31th Workshop on Geothennal Reservoir Engineering, Stanford University, Stanford, USA.
Meju, M.A., 2002. Geoelectromagnetic exploration for natural resources: models, case studies and challenges. Surv. Geophys. 23, 133–205.
Mogi, T., Nakama, S., 1993. Magnetotelluric interpretation of the geothermal system of the Kuju volcano, southwest Japan. J. Volcanol. Geotherm. Res. 56, 297–308.
Mulyadi, 2000. Magnetic Telluric method applied for geothermal exploration in Sibayak, North Sumatra. Proc. World Geothermal Congress, Kyushu-Tohoku, Japan, pp. 1469–1472.
Natland, J.-H., Dick, H.J.B., 2001. Formation of the lower ocean crust and the crystallization of gabbroic cumulates at a very slowly spreading ridge. J. Volcanol. Geotherm. Res. 110, 191–233.
Okada, H., Yasuda, Y., Yagi, M., Kai, K., 2000. Geology and fluid chemistry of the Fushime geothermal field, Kyushu, Japan. Geothermics 29, 279–311.
Oskooi, B., Pedersen, L.B., Smirnov, M., Árnason, K., Eysteinsson, H., Manzella, A., 2005. The deep geothermal structure of the Mid-Atlantic Ridge deduced from MT data in SW Iceland. Phys. Earth Planet. Inter. 150, 183–195.
Patrier, P., Papapanagiotou, P., Beaufort, D., Traineau, H., Bril, H., Rojas, J., 1996. Role of permeability versus temperature in the distribution of the fine (<0.2 mu m) clay fraction in the Chipilapa geothermal system (El Salvador, Central America). J. Volcanol. Geotherm. Res. 72, 101–120.
Pellerin, L., Johnston, J.M., Hohmann, G.W., 1996. A numerical evaluation of electromagnetic methods in geothermal exploration. Geophysics 61, 121–130.
Pérez-Flores, M.A., Gomez-Treviño, E., 1997. Dipole–dipole resistivity imaging of the Ahuachapan–Chipilapa geothermal field, El Salvador. Geothermics 26 (5/6), 657–680.
Pérez-Flores, M.A., Schultz, A., 2002. Application of 2-D inversion with genetic algorithms to magnetotelluric data from geothermal areas. Earth Planets Space 54, 607–616.
Pérez-Flores, M.A., Antonio-Carpio, R.G., Gomez-Treviño, E., 2005. Tridimensional inversion of DC resistivity data. Proceedings World Geothermal Congress, Antalya, Turkey.
Risk, G.F., Bibby, H.M., Bromley, C.J., Caldwell, T.G., Bennie, S.L., 2002. Appraisal of the Tokaanu-Waihi geothermal field and its relationship with the Tongariro geothermal field, New Zealand. Geothermics 31, 45–68.
Romo, J.M., Flores, C., Vega, R., Vázquez, R., Pérez Flores, M.A., Treviño, E.G., Esparza, F.J., Quijano, J.E., García, V.H., 1997. A closely-spaced magnetotelluric study of the Ahuachapan–Chipilapa geothermal field, El Salvador. Geothermics 26, 627–656.
Romo, J.M., Wong, V., Flores, C., 2000. The subsurface electrical conductivity and the attenuation of coda waves at Las Tres Virgines geothermal field in Baja California Sur, Mexico, 2000. Proc. World Geothermal Congr., Kyushu-Tohoku, Japan, pp. 1645–1650.
Sasaki, Y., Meju, M.A., 2006. Three-dimensional joint inversion for magnetotelluric resistivity and static shift distributions in complex media. J. Geophys. Res. 111, B05101. doi:10.1029/2005JB004009.
Sener, M., Gevrek, A.I., 2000. Distribution and significance of hydrothermal alteration minerals in the Tuzla hydrothermal system, Canakkale, Turkey. J. Volcanol. Geotherm. Res. 96, 215–228.
Shankland, T., Ander, M., 1983. Electrical conductivity, temperatures, and fluids in the lower crust. J. Geophys. Res. 88 (B11), 9475–9484.
Shen, J., Sasaki, Y., Ushijima, K., 2000. Reconstruction of resistivity and permittivity profiles using electromagnetic well logging data. Proc. World Geothermal Congress, Kyushu-Tohoku, pp. 1731–1736.
Shmonov, V.M., Vitovtova, V.M., Zharikov, A.V., 2000. Fluid permeability of the earth crust rocks (in Russian). Scientific World, Moscow. 276 pp.
Spichak, V.V., 2001. Three-dimensional interpretation of MT data in volcanic environments (computer simulation). Ann. Geofis. 44 (2), 273–286.
Spichak, V.V., 2002. Advanced three-dimensional interpretation technologies applied to the MT data in the Minamikayabe thermal area (Hokkaido, Japan). Expanded abstr. EAGE 64th Conference, Florence, Italy.
Spichak, V.V., Popova, I.V., 2000. Artificial neural network inversion of MT — data in terms of 3D earth macro-parameters. Geophys. J. Int. 42, 15–26.
Spichak, V.V., Fukuoka, K., Kobayashi, T., Mogi, T., Popova, I., Shima, H., 1999a. Neural - network based interpretation of insufficient and noisy MT data in terms of the target macro-parameters. Expanded abstr. II Symp. on 3D Electromagnetics, Salt Lake city, USA, pp. 297–300.
Spichak, V.V., Menvielle, M., Roussignol, M., 1999b. Three-dimensional inversion of MT data using Bayesian statistics. In: Spies, B., Oristaglio, M. (Eds.), 3D Electromagnetics, SEG monograph, GD7, Tulsa, USA, pp. 406–417.
Spichak, V., Rybin, A., Batalev, V., Sizov, Yu., Zakharova, O., Goidina, A., 2006. Application of ANN techniques to combined analysis of magnetotelluric and other geophysical data in the northern Tien Shan crustal area. Extended Abstract 18th IAGA WG 1.2 Workshop on Electromagnetic Induction in the Earth, El Vendrell, Spain.
Spichak, V.V., Borisova, V.P., Fainberg, E.B., Khalezov, A.A., Goidina, A.G., 2007a. Electromagnetic 3D tomography of the Elbrus volcanic center according to magnetotelluric and satellite data. J. Volcanol. Seismol. 1 (1), 53–66.
Spichak, V.V., Schwartz, Ya., Nurmukhamedov, A., 2007b. Conceptual model of the Mutnovsky geothermal deposit (Kamchatka) based on electromagnetic, gravity and magnetic data. Expanded abstr. EAGE Workshop on Innovation in EM, Gravity and Magnetic methods: a new perspective for exploration, Capri, Italy.
Spichak, V.V., Zakharova, O.K., Rybin, A.K., 2007c. Estimation of the sub-surface temperature by means of magnetotelluric sounding. Expanded abstr. XXXII Workshop on Geothermal Reservoir Engineering, Stanford University, Stanford, USA.
Srodon, J., 1999. Nature of mixed-layer clays and mechanisms of their formation and alteration. Annu. Rev. Earth Planet. Sci. 27, 19–53.
Suharno, S., Browne, P.R.L., Soengkono, S., Prijanto, Sudarman, S., 2000. A geophysical model and the subsurface geology at the Ulubelu geothermal area, Lampung, Indonesia. Abstract. AAPG Bulletin, vol. 84, p. 1498.

Svetov, B., 2006. Seismoelectric methods of Earth study. In: Spichak, V.V. (Ed.), Electromagnetic Sounding of the Earth's Interior. Elsevier, Amsterdam, pp. 79–101.
Takasugi, S., Tanaka, K., Kawakami, N., Muramatsu, S., 1992. High spatial resolution of the resistivity structure revealed by a dense network MT measurement — a case study in the Minamikayabe Area, Hokkaido, Japan. Geomagn. Geoelectr. 44, 289–308.
Talebi, B., Khosrawi, K., Ussher, G., 2005. Review of resistivity surveys from the NW Sabalan geothermal field, Iran. Proc. World Geothermal Congress, Antalia, Turkey.
Uchida, T., 1995. Resistivity structure of Sumikawa geothermal field, northeastern Japan, obtained from magnetotelluric data. Proc. World Geothermal Congress, Florence, Italy, pp. 921–925.
Uchida, T., 2005. Three-dimensional magnetotelluric investigation in geothermal fields in Japan and Indonesia. Proc. World Geothermal Congress, Antalia, Turkey.
Uchida, T., Ogawa, Y., Takakura, S., Mitsuhata, Y., 2000. Geoelectrical investigation of the Kakkonda geothermal field, northern Japan. Proc. World Geothermal Congress, Kyushu-Tohoku, Japan, pp. 1893–1898.
Uchida, T., Song, Y., Lee, T.J., Mitsuhata, Y., Lim, S.K., Lee, S.K., 2005. Magnetotelluric survey in an extremely noisy environment at the Pohang low-enthalpy geothermal area, Korea. Proc. World Geothermal Congress, Antalia, Turkey.
Ushijima, K., Noritomi, K., Tagomori, K., Kinoshita, Y., 1986. Joint inversion of MT and DC resistivity data at Hatchobaru area. Geotherm. Resour. Council Trans. 10, 243–246.
Ushijima, K., Mustopa, E.J., Jotaki, H., Mizunaga, H., 2005. Magnetotelluric soundings in the Takigami geothermal Aria, Japan. Proc. World Geothermal Congress, Antalia, Turkey.
Ussher, G., Harvey, C., Johnstone, R., Anderson, E., 2000. Understanding the resistivities observed in geothermal systems. Proc. World Geothermal Congress, Kyushu-Tohoku, Japan, pp. 1915–1920.
Varentsov, Iv.M., 2006. Arrays of simultaneous electromagnetic soundings: design, data processing and analysis. In: Spichak, V.V. (Ed.), Electromagnetic Sounding of the Earth's Interior. Elsevier, Amsterdam, pp. 259–273.
Veeraswamy, K., Harinarayana, T., 2006. Electrical signatures due to thermal anomalies along mobile belts reactivated by the trail and outburst of mantle plume: evidences from the Indian subcontinent. J. Appl. Geophys. 58 (4), 313–320.
Volpi, G., Manzella, A., Fiordelisi, A., 2003. Investigation of geothermal structures by magnetotellurics (MT): an example from the Mt. Amiata area, Italy. Geothermics 32, 131–145.
Wannamaker, P.E., 1986. Electrical conductivity of water-undersaturated crustal melting. J. Geophys. Res. 91 (B6), 6321–6327.
Wannamaker, P.E., 1997a. Tensor CSAMT survey over the Sulphur Springs thermal area, Valles Caldera, New Mexico, U.S.A, Part I: Implications for structure of the western caldera. Geophysics 62, 451–465.
Wannamaker, P.E., 1997b. Tensor CSAMT survey over the Sulphur Springs thermal area, Valles Caldera, New Mexico, U.S.A, Part II: Implications for CSAMT methodology. Geophysics 62, 466–476.
Wannamaker, P.E., Jiracek, G.R., Stodt, J.A., Caldwell, T.G., Gonzales, V.M., McKnight, J.D., Porter, A.D., 2002. Fluid generation and pathways beneath an active compressional orogen, the New Zealand southern Alps, inferred from magnetotelluric data. J. Geophys. Res. 107 (6), 6–1 – 6-22.
Wannamaker, P.E., Rose, P.E., Doemer, W.M., McCulloch, J., Nurse, K., 2005. Magnetotelluric surveying and monitoring at the Coso geothermal area, California. Support of the Enhanced Geothermal Systems Concept: Survey Parameters, Initial Results. Proc. World Geothermal Congress, Antalia, Turkey.
Ward, S.H., 1990. Resistivity and induced polarization methods. In: Ward, S.H. (Ed.), Geotechnical and environmental geophysics, vol. 1 – Review and tutorial, Soc. Explor. Geophys, pp. 147–189.
Waxman, M.H., Smith, J.M., 1968. Electrical conductivities in oil-bearing shaley sands. Soc. Pet. Eng. J. 102–122 SPE Paper 1863-A at SPE Ann. Fall Meeting, Houston.
Yamane, K., Ohsatu, K., Ohminato, T., Kim, H.J., 2000. Three-dimensional magnetotelluric investigation in Kakkonda geothermal area, Japan. Proc. World Geothermal Congress, Kyushu-Tohoku, Japan, pp. 1965–1968.
Yang, K., Huntington, J.F., Browne, P.R.L., Ma, C., 2000. An infrared spectral reflectance study of hydrothermal alteration minerals from the Te Mihi sector of the Wairakei geothermal system, New Zealand. Geothermics 29, 377–392.
Yang, K., Browne, P.R.L., Huntington, J.F., Walshe, J.L., 2001. Characterising the hydrothermal alteration of the Broadlands–Ohaaki geothermal system, New Zealand, using short-wave infrared spectroscopy. J. Volcanol. Geotherm. Res. 106, 53–65.
Zhang, S., Paterson, M.S., Cox, S.F., 1994. Porosity and permeability evolution during hot isostatic pressing of calcite aggregates. J. Geoph. Res. 99, 15741–15760.
Zlotnicki, J., Vargemezis, G., Mille, A., Bruere, F., Hammouya, G., 2006. State of the hydrothermal activity of Soufriere of Guadeloupe volcano inferred by VLF surveys. J. Appl. Geophys. 58 (4), 265–279.